

Chapter 7 Characterisation of the Pleistocene minerogenic sediments of the Gordano Valley

7.1 Introduction

This chapter addresses the third objective: to characterise the Pleistocene sediments and interpret their depositional environments. This is achieved through the techniques discussed in Chapter 4 (section 4.12) and both depositional and post-depositional environments are interpreted. An assessment of particle size summary statistics is followed by bivariate plots of particle size parameters, segment analysis, bivariate plots of gravel clast shape and roundness data and gravel clast shape histograms. This information is then combined with lithological evidence and palaeontological evidence (Chapter 6, sections 6.4 and 6.9) to infer a depositional history of the sediments. Stratigraphical (Chapter 6, section 6.2) and geochemical (section 6.7) evidence is then interpreted to infer post-depositional environments. Finally, the geochronological evidence is discussed and interpreted.

7.2 Characterisation of sedimentary attributes to determine the Pleistocene depositional environments

A preliminary assessment of depositional environments is possible from examination of the particle size data presented in section 6.3, indicating the likelihood or otherwise of some depositional environments; these are summarised in Table 7.1.

Table 7.1: Preliminary assessment of depositional environments from particle size data (source: Reineck & Singh 1973)

Depositional environment	Units	Basis
<i>Not aeolian</i>	GV3, GV4, GV5, GV6, GV9, GV10, GV11, PG7, PGA1, PGA2, PGA3, PGA14, CGA3, CGA4, CGA5, CGA6, CGA7, CGA12, CGA13, CGA14, CGB1, CGB2, CGB3, CGB7, CGB9, CGB13, NR2, NR3, NR4, NR5, NR6, NR7, NR9, NR13, NR14, NR15, NR16, NR21, NR24, CM2, CM3, CM4, CM8, TG2, TG3, TG8, TG9, TG12, TG13, TG14	Particle size
	PGA13, PGA15, PGA16, PGA17, CGB5, NR1, NR10, NR11	Skewness
<i>Not beach</i>	GV2, GV3, GV4, GV5, GV6, GV9, GV10, all units of core PG, PGA1 to PGA14, all units of core CGB, all units of core CM	Very poor sorting (σ 2-4)
	All units of core CGA except CGA14	Very poor sorting (σ 2-4) and skewness of <1
	All units of cores NR and TG	Extremely poor sorting (σ 1.3 - >4.0)
<i>Not dune</i>	GV7, all units of core PG, PGA4, PGA6, PGA7, PGA8, PGA9, PGA10, PGA11, PGA12, CGA1, CGA2, CGA8, CGA9, CGA10, CGA11	Very poor sorting (σ 2-4)
	All units of core NR, all units of core TG	Extremely poor sorting (σ 1.3 - >4.0)
Fluvial	GV11, CGA4, CGB2, NR3, NR4, NR5, NR6, NR14, NR15, NR16, CM3, TG9, TG13	Bimodal particle size distribution and positive skewness
	CGA14	Moderate sorting and positive skewness

7.2.1 Bivariate plots of particle size parameters

Bivariate of particle size moments skewness against kurtosis (Figure 7.1) was used to differentiate river, beach and aeolian/settling depositional characteristics. Aeolian or settling deposition is indicated for fifty six units including a large number of gravel units, such as CGB7, CGB13, NR16 and TG13; this probably reflects the depositional environment of the gravel matrix.

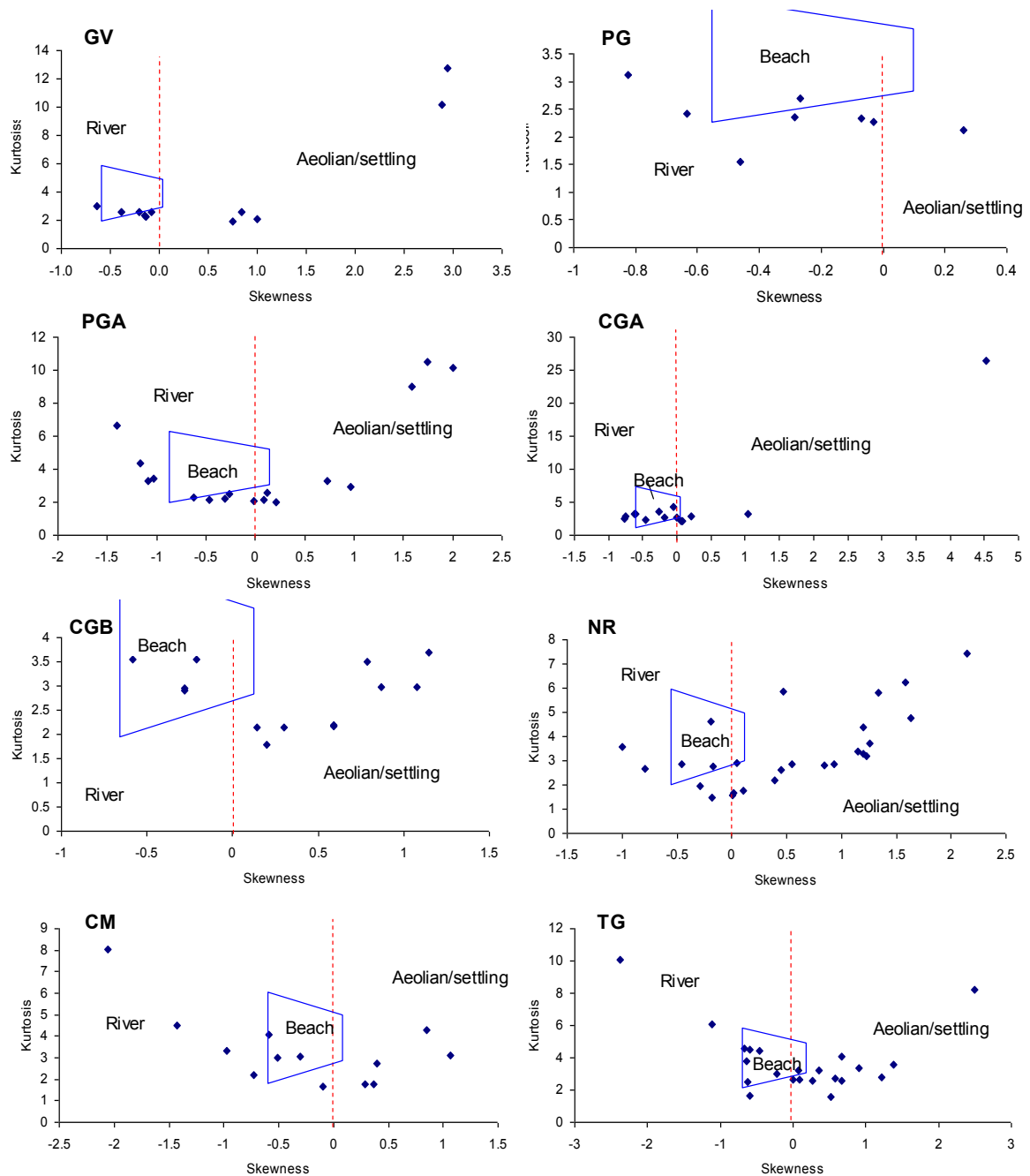


Figure 7.1: Bivariate plots of sediment skewness against kurtosis (adapted from Tanner 1991). GV: GV1 plots as a beach deposit. PG: PG7 plots as an aeolian/settling deposit; PG1 plots as a beach deposit. PGA: Eight units plot as aeolian/settling deposits; PGA6 and PGA12 plot as beach deposits. CGA: Six units plot as aeolian/settling deposits; five units plot as beach deposits. All other units in GV, PG, PGA and CGA plot as river deposits. CGB: Four units plot as beach deposits (two plots coincide on the diagram). NR: Four units plot as river deposits, four more units plot as beach deposits, NR19 and NR24 plot on the boundary between river and aeolian deposition. CM: Three units plot as beach deposits. TG: Three units plot as river deposits, seven units plot as beach deposits. All other units in CGB, NR, CM and TG plot as aeolian or settling deposits; two plots coincide on the diagram for CGB

Fluvial deposition is indicated for thirty one units; two units (NR19 and NR24) plot on the boundary between river and aeolian deposition. Beach deposition is indicated for twenty six units. The depositional characteristics indicated are summarised in Table 7.2.

Table 7.2: Summary of depositional environments indicated by bivariate of particle size moments skewness against kurtosis

Depositional environment	Units
Aeolian/settling	GV3, GV4, GV5, GV11, PG7, PGA1, PGA2, PGA3, PGA4, PGA8, PGA15, PGA16, PGA17, CGA3, CGA4, CGA5, CGA6, CGA14, CGB1, CGB2, CGB3, CGB4, CGB5, CGB6, CGB7 (CGB4 and CGB7 coincide on the diagram), CGB9, CGB13, NR1, NR2, NR4, NR5, NR6, NR7, NR9, NR10, NR11, NR12, NR13, NR14, NR15, NR16, NR21, NR26, TG2, TG3, TG4, TG5, TG8, TG9, TG12, TG13, TG14, TG17, TG19, TG21.
Fluvial	GV1, GV6, GV7, GV8, GV9, PG2, PG3, PG4, PG5, PG6, PG8, PGA5, PGA10, PGA11, PGA13, CGA2, CGA7, CGA8, NR17, NR18, NR20, NR22, CM1, CM5, CM6, CM7, CM9, TG1, TG6, TG10, TG15
Beach	GV1, PG1, PGA6, PGA12, CGA1, CGA9, CGA11, CGA12, CGA13, CGB8, CGB10, CGB11, CGB12 (CGB11 and CGB12 coincide on the diagram), NR3, NR8, NR23, NR25, CM10, CM12, CM13, TG7, TG11, TG16, TG18, TG20, TG22

Bivariate of mean particle size against sorting for the $>4 \phi$ fraction of sediments was used to differentiate between river and closed basin/settling depositional environments. Figure 7.2 shows that all Gordano Valley sediments demonstrate river or closed basin/settling depositional characteristics; plots cluster close to the river environmental envelope, with most units plotting in the closed basin/settling environmental envelope. This indicates that for most units deposition was in a closed basin-type environment with a nearby river. CGA14 plots furthest from the river envelope, suggesting a diminished fluvial influence in its depositional environment. Fluvial deposition is indicated for units GV1, GV2, GV5, GV8, NR11, NR16, NR19, NR23 and TG1, which plot within the river depositional envelope.

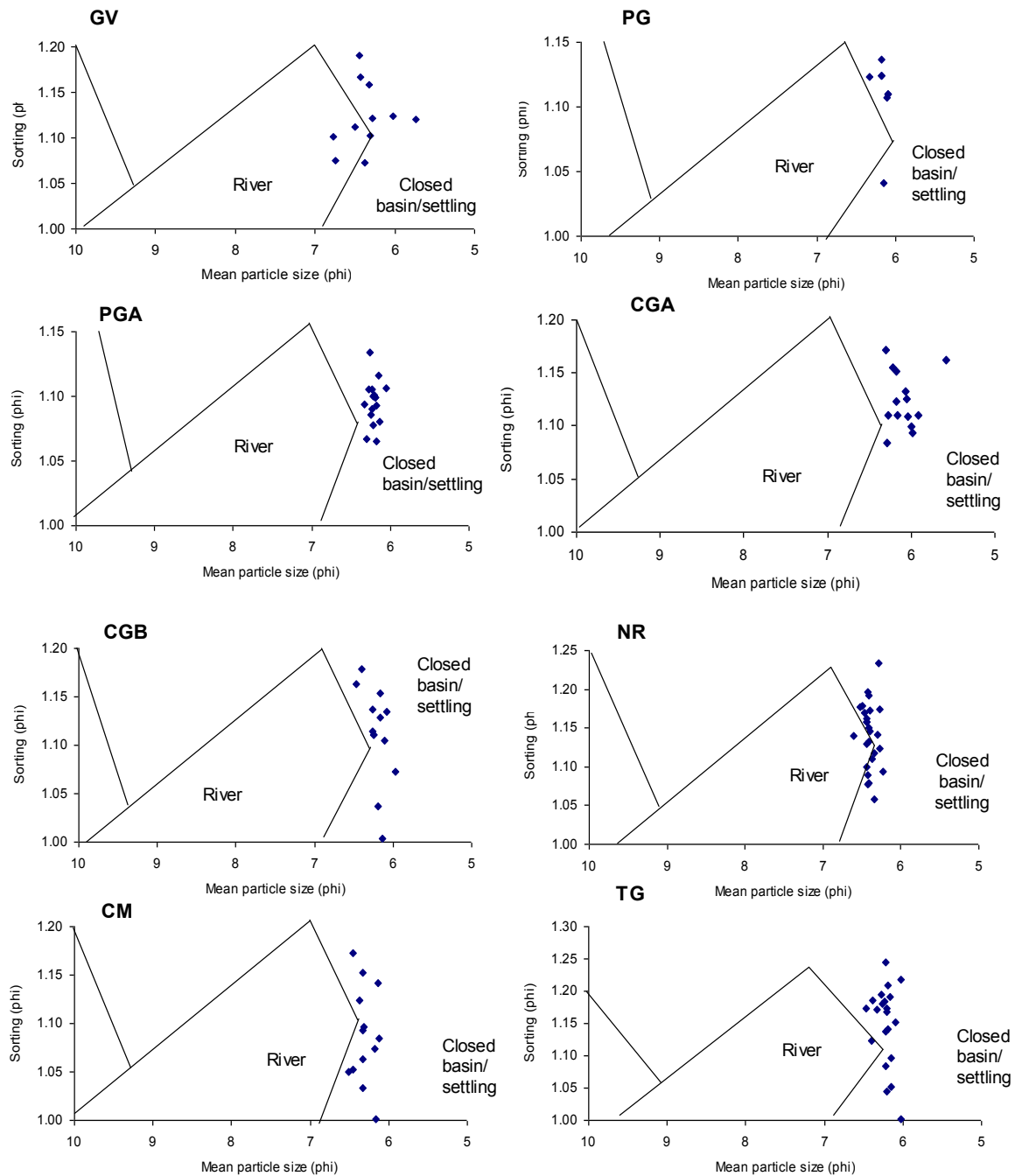


Figure 7.2: Bivariate plots of mean particle size against sorting for the $>4 \phi$ fraction (adapted from Lario *et al.* 2002). The plots cluster around the closed basin/settling depositional envelope, close to the river envelope; units, GV1, GV2, GV5, GV8, NR11, NR16, NR19, NR23 and TG11 plot within the river depositional envelope

Bivariance of median particle size against skewness and of median particle size against sorting was used to differentiate between river, wave and quiet water depositional characteristics. The plots of median particle size against skewness (Figure 7.3) show that

thirty two units plot in the river depositional envelope, sixteen units plot in the wave environmental envelope, NR23 and CM9 plot in the overlap between the river and wave envelopes and GV6 plots close to the wave envelope. CGB4, CGB5 NR10, NR11 and NR26, plot in the quiet water, slow deposition envelope and CM11 plots on the boundary for quiet water, slow deposition. Just over half the units plot outside any of the recognised environmental envelopes; CGA4 plots on its own on the left of the CGA diagram and CGA14 plots on its own at the top of the diagram.

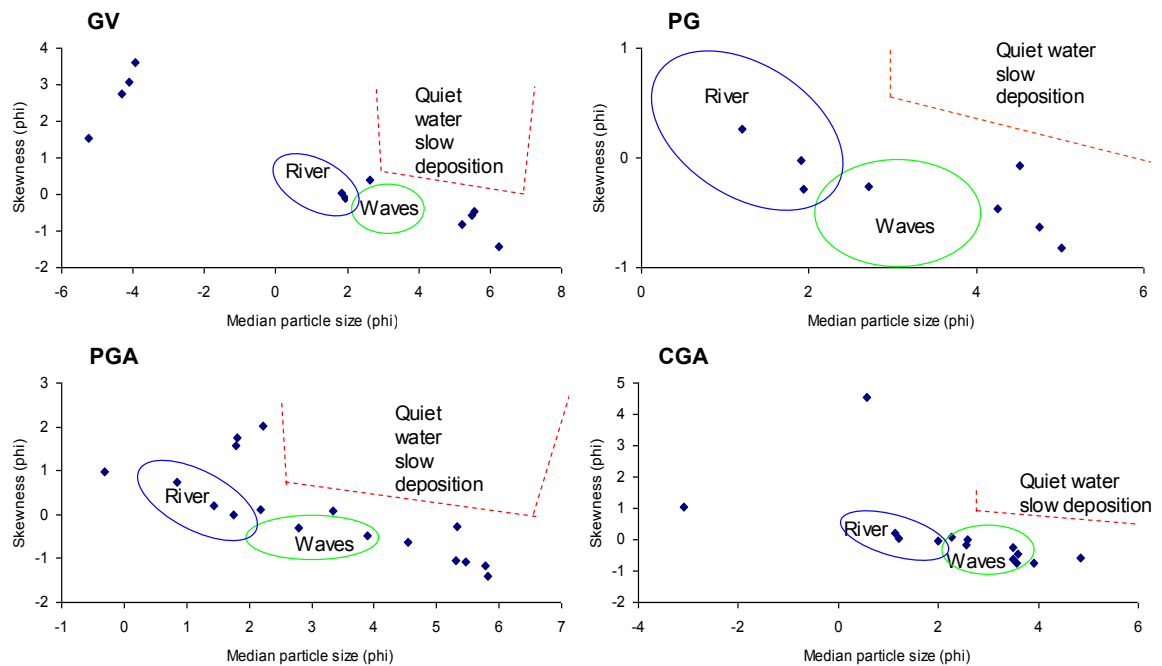


Figure 7.3: Bivariate plots of sediment median particle size against skewness (adapted from Stewart 1958). GV: GV9 and GV10 plot in the river environmental envelope. PG: Three units plot in the river environmental envelope; PG1 plots in the waves envelope. PGA: Three units plot in the river environmental envelope; two units plot in the waves environmental envelope. CGA: Three units plot in the river environmental envelope; six units plot in the waves envelope; CGA4 plots on its own on the left of the diagram; CGA14 plots on its own at the top of the diagram. All other units plot outside the environmental envelopes

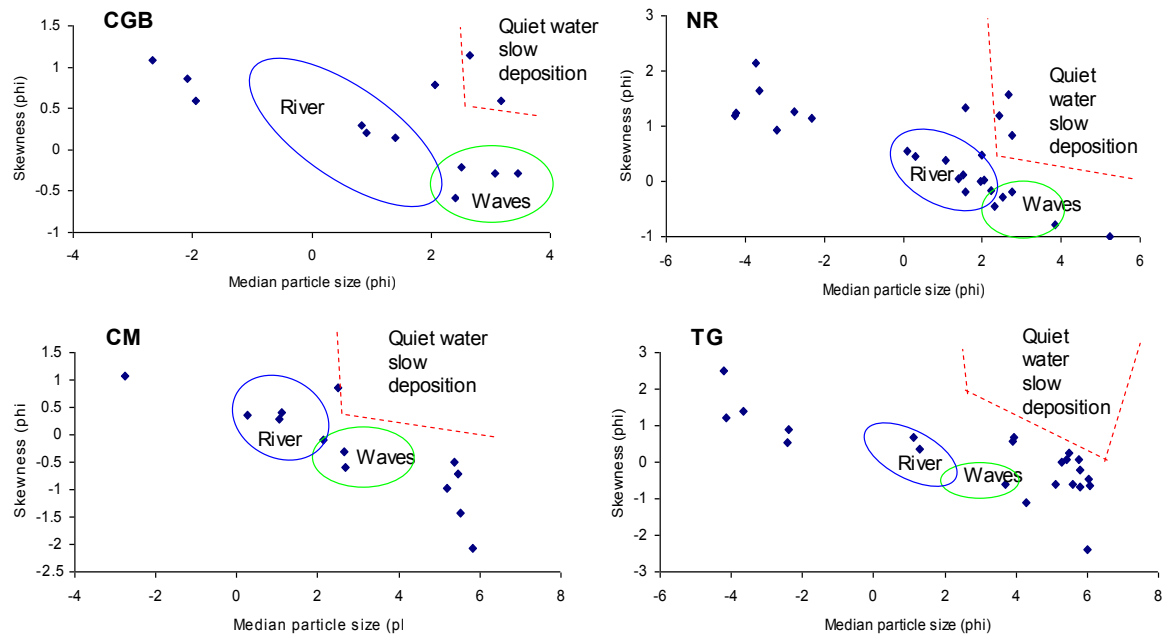


Figure 7.3 (continued): Bivariate plots of sediment median particle size against skewness. CGB: Three units plot in the river environmental envelope; four units plot in the waves envelope; CGB4 and CGB5 plot in the quiet water envelope. NR: Nine units plot in the river environmental envelope; four units plot in the waves environmental envelope; NR23 plots in the overlap between the river and waves envelopes; three units plot in the quiet water, slow deposition envelope. CM: Three units plot in the river environmental envelope; CM10 and CM12 plot in the waves envelope; CM9 plots in the overlap between the two environments. TG: TG8 and TG12 plot in the river environmental envelope; TG20 plots in the waves environmental envelope. All other units plot outside the environmental envelopes

However, plots of median particle size against sorting (Figure 7.4) show that no units plot in the waves envelope, and only CGA14 plots in the rivers envelope, whilst thirty four units plot in the quiet water, slow deposition envelope, with GV6, GV9 and GV10 plotting close to this envelope. Most units again plot outside the environmental envelopes with CGA4 again plotting on its own on the left of the diagram.

The depositional characteristics indicated by bivariate of median particle size against skewness and of median particle size against sorting are summarised in Table 7.3.

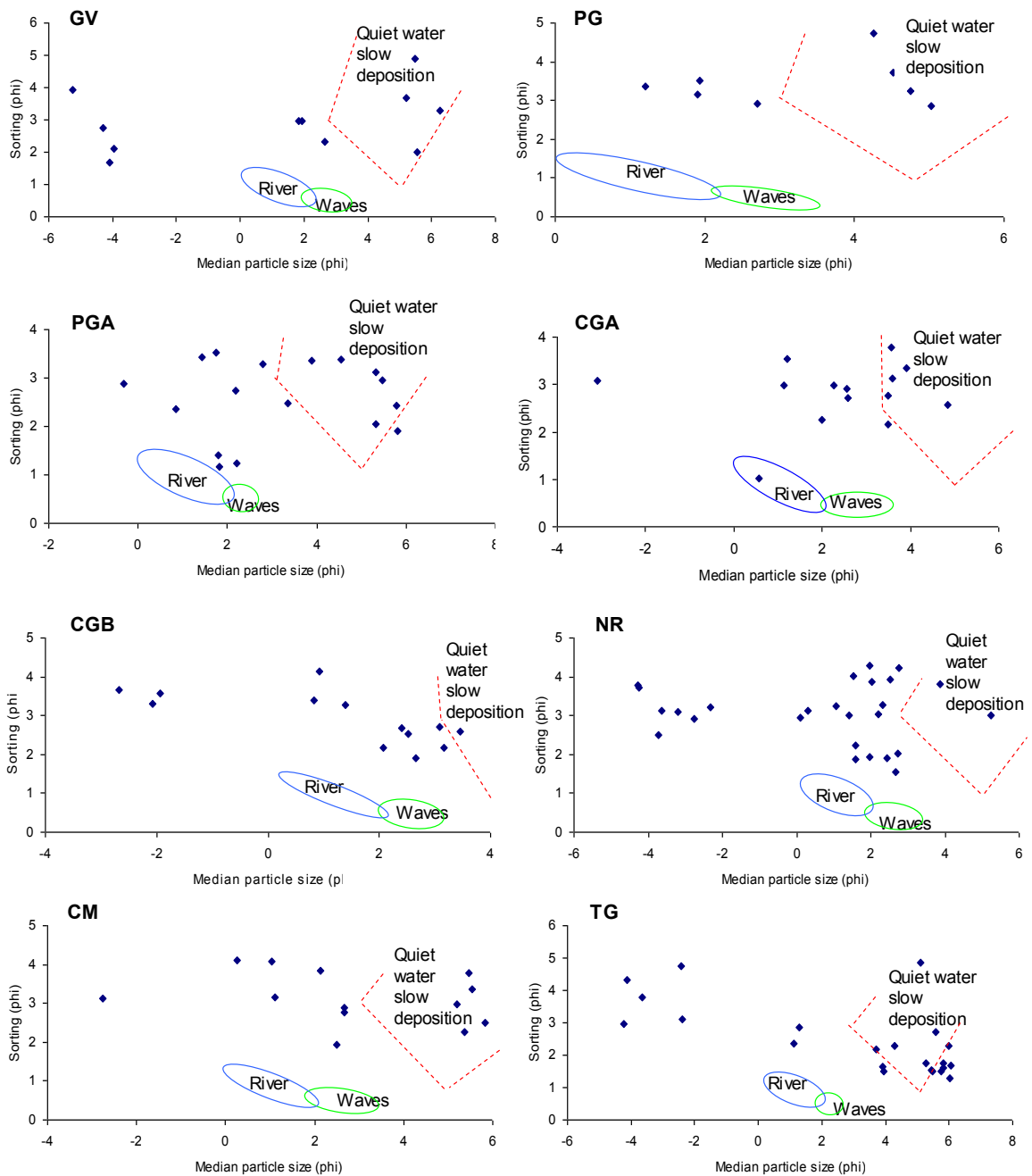


Figure 7.4: Bivariate plots of sediment median particle size against sorting (adapted from Stewart 1958). GV: Four units plot in the quiet water, slow deposition environmental envelope. PG: Four units plot in the quiet water, slow deposition environmental envelope. PGA: Six units plot in the quiet water, slow deposition environmental envelope. CGA: CGA14 plots in the river environmental envelope; five units plot in the quiet water slow, deposition environmental envelope; CGA4 plots on its own on the left of the diagram, outside the environmental envelopes. CGB: CGB11 plots in the quiet water, slow deposition environmental envelope. NR: NR20 and NR22 plot in the quiet water, slow deposition envelope. CM: Five units plot in the quiet water, slow deposition environmental envelope. TG: Seven units plot in the quiet water, slow deposition envelope. All other units plot outside the environmental envelopes

Table 7.3: Summary of depositional environments indicated by bivariance of median particle size against skewness and of median particle size against sorting

Indicator	Depositional environment	Units
Median particle size against skewness	River	GV9, GV10, PG4, PG7, PG8, PGA1, PGA3, PGA14, CGA5, CGA6, CGA13, CGB3, CGB9, CGB13, CGB8, CGB10, CGB11, CGB12, NR3, NR5, NR7, NR8, NR12, NR13, NR19, NR21, NR24, CM2, CM4, CM8, TG8, TG12
	Waves	PG1, PGA7, PGA9, CGA1, CGA2, CGA3, CGA10, CGA11, CGA12, NR17, NR18, NR22, NR25, CM10, CM12, TG20
	Quiet water, slow deposition	CGB4, CGB5, NR10, NR11, NR26
Median particle size against sorting	River	CGA14
	Quiet water, slow deposition	GV1, GV2, GV7, GV8, PG2, PG3, PG5, PG6, PGA6, PGA9, PGA10, PGA11, PGA12, PGA13, CGA2, CGA7, CGA8, CGA9, CGA11, CGB11, NR20, NR22, CM1, CM5, CM6, CM7, CM13, TG4, TG10, TG11, TG15, TG18, TG20, TG21

Bivariance of median particle size against the particle size of the coarsest one percentile was used to differentiate between mudflow, river channel and braided stream depositional characteristics. The pattern of plots shown in Figure 7.5 suggests water-lain deposition for most units and indicates mudflow characteristics for twenty units, and probably also PG5, PG6, CGA7 and NR22 which plot just outside the lower end of the mudflow depositional envelope, indicating higher competence of the transporting agent (Bull 1962). Braided stream deposition is indicated for twenty six units; the proximity of CGA14 to the $x = y$ line indicates its better sorting (Bull 1962) and although it falls outside the known envelope for braided stream deposition, probably still represents deposition by braided stream. PGA8, CGA3 and CGB6 could be either braided stream or river channel deposits as they plot in the overlap between the two environments.

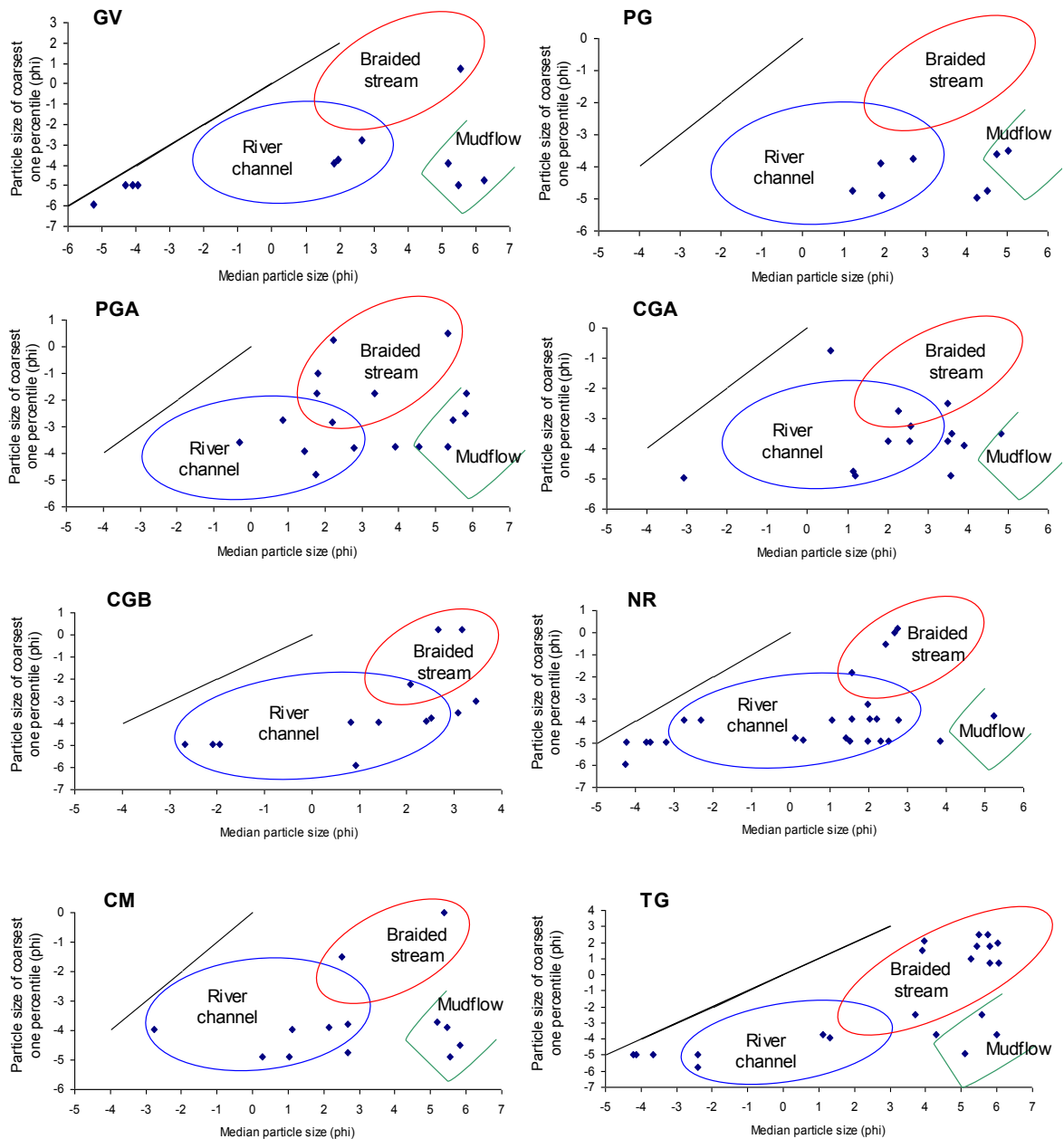


Figure 7.5: Bivariate plots of median particle size against the particle size of the coarsest one percentile (adapted from Bull 1962). GV: Three units plot as mudflow deposits, GV7 plots as a braided stream deposit and four units plot outside the environmental envelopes. PG: PG2 and PG3 plot as mudflow deposits; PG5 and PG6 are also probably mudflow deposits as they plot marginally to the mudflow envelope. PGA: Five units plot as braided stream deposits, PGA8 plots in the overlap between braided stream and river channel deposition, five units plot as mudflow deposits, PGA9 plots outside the environmental envelopes, intermediate between the mudflow and river channel envelopes. CGA: CGA9 plots as a mudflow deposit; CGA7 plots marginally to the mudflow envelope and is also probably a mudflow deposit; CGA1 plots as a braided stream deposit; CGA3 plots in the overlap between braided stream and river channel deposit; three units plot as intermediate between mudflow and river channel environments; CGA4, CGA7 & CGA14 plot outside the environmental envelopes. CGB: CGB4 and CGB5 plot as a braided stream deposits; CGB6 plots

in the overlap between braided stream and river channel deposits; CGB11 and CGB12 plot outside the environmental envelopes. NR: NR20 plots as a mudflow deposit, four units plot as braided stream deposits, five units plot outside the environmental envelopes. CM: CM11 and CM13 plot as a braided stream deposits, four units plot as mudflow deposits, CM12 plots just outside the environmental envelope for river channel deposition. TG: Four units plot as mudflows, three units plot beyond the end of the river channel envelope; eleven units plot as braided stream deposits; four units plot as river channel deposits

River channel characteristics are indicated for fifty one units; this probably extends to GV3, GV4, GV5 and GV11, CGA4, NR2, NR9, NR15 and NR16, TG2, TG3, and TG14 which plot outside the left-hand side of the river channel envelope, indicating higher competence of the transporting agent (Bull 1962), suggesting deposition from a turbulent river. CM12 plots just outside the opposite end of the environmental envelope for river channel deposition, suggesting deposition from a quieter stream. PGA9, CGA2, CGA8 and CGA11 plot intermediate between the mudflow and river channel envelopes, TG10 plots intermediate between mudflow and braided stream deposition and CGB11 and CGB12 plot between the environmental envelopes for mudflow, braided stream and river channel deposition. Table 7.4 provides as summary of the characteristics indicated.

7.2.2 Segment analysis

Segment analysis (section 4.12.1) of particle size data was used to separate sediments into sandy river, dune or river silts/closed basin groups. These are shown in Figure 7.6. The depositional environments indicated are summarised in Table 7.5.

The sediments of core GV separate into four groups: a sandy river group (GV10, probably also GV4 and GV5), a river silts and clays or closed basin group (GV7, probably also GV6 and GV9), which has some overlap with a dune group (GV6). The fourth group falls outside the parameters of the segments and is divided into two sub-groups: one which plots in the coarse tail close to the sandy river envelope, comprises gravel units and probably represents a fluvial gravel population (GV3 and GV11) and another which plots closest to the river silts and dune segments (GV1, GV2 and GV8).

Table 7.4: Summary of depositional environments indicated by bivariance of median particle size against the particle size of the coarsest one percentile

Depositional environment	Units
Mudflow	GV1, GV2, GV8 PG2, PG3, probably PG5, PG6 PGA5, PGA10, PGA11, PGA12, PGA13 CGA9, probably CGA7 NR20, probably NR22 CM1, CM5, CM6, CM7 TG1, TG10, TG11, TG15
River channel	GV6, GV9, GV10, probably GV3, GV4, GV5, GV11 PG1, PG4, PG7, PG8 PGA1, PGA2, PGA3, PGA7, PGA14 CGA5, CGA6, CGA10, CGA12, CGA13, probably CGA4 CGB1, CGB2, CGB3, CGB7, CGB8, CGB9, CGB 10, CGB13 NR3, NR4, NR5, NR6, NR7, NR8, NR12, NR13, NR14, NR17, NR18, NR19, NR21, NR23, NR24, NR25, probably NR2, NR9, NR15 & NR16 CM2, CM3, CM4, CM8, CM9, CM10 TG8, TG9, TG12, TG13 probably TG2, TG3, TG14
Braided stream	GV7 PGA4, PGA6, PGA15, PGA16, PGA17 CGA1, probably CGA14 CGB4, CGB5 NR1, NR10, NR11, NR26 CM11, CM13 TG4, TG5, TG6, TG7, TG16, TG17, TG18, TG19, TG20, TG21, TG22

The sediments of core PG separate into three groups: a sandy river group (PG7, probably also PG8), a dune group (PG1 and PG4) and a group which falls outside the segments, but which plots closest to the river silts segment (PG2, PG3, PG5 and PG6).

Core PGA sediments separate into five groups: a 'No tail' group, representing a beach environment (PGA15, PGA16 and PGA17), a sandy river group (PGA1, PGA2, PGA14), a river silts and clays or closed basin group (PGA4, PGA5, PGA6 and PGA10), a dune group (PGA7), and a group that plots outside the parameters of the segments (PGA9, PGA11, PGA12 and PGA13). PGA3 which plots marginally to the boundary of the sandy

river segment and PGA8 which plots on the boundary between sandy river and dune environments probably form part of the sandy river group.

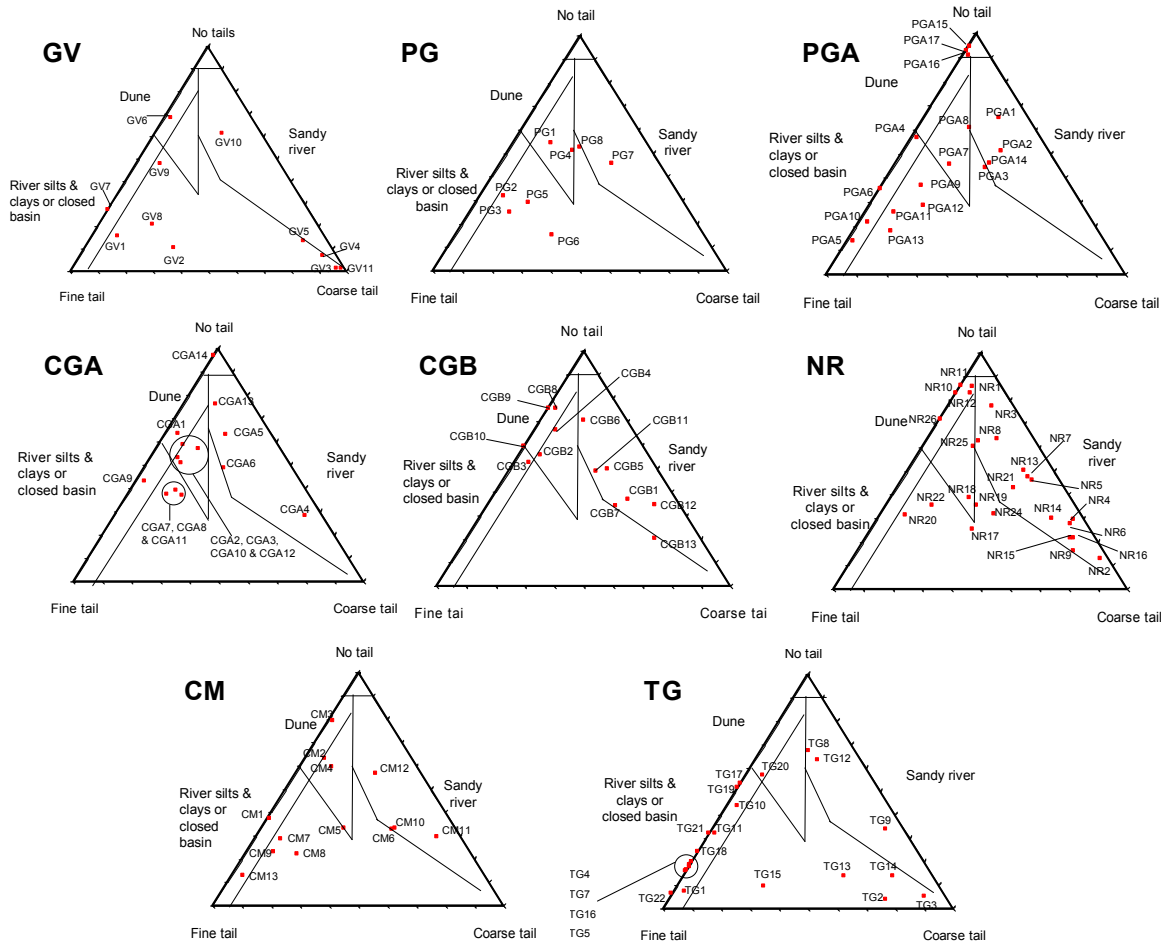


Figure 7.6: Segment analysis of the Gordano Valley sediments (adapted from Tanner 1991). GV: GV6 plots as either a dune or river silts & clays or closed basin deposit; seven units plot outside the segment parameters. PG: PG8 plots between dune and sandy river deposits, slightly closer to the sandy river segment; four units plot outside the segment parameters. PGA: PGA8 plots on the boundary between sandy river and dune environments and PGA3 plots marginally to the boundary of the sandy river segment. CGA: CGA1 plots as either dune or river silts & clays or closed basin deposits; three units plot outside the segment parameters. CGB: CGB8, CGB9 and CGB10 plot as either dune or river silts & clays or closed basin deposits; CGB13 plots marginally outside the sandy river segment. NR: Five units plot in the overlap between dune deposits and those of river silt and clay or closed basin deposits. CM: CM3 plots as either dune or river silts & clays or closed basin deposits; three units plot outside the segment parameters. TG: TG20 plots in the overlap between dune deposits and those of river silt and clay or closed basin deposits

Core CGA sediments separate into five groups: a sandy beach (no tail) group (CGA14), a sandy river group (CGA4, CGA5, CGA6 and CGA13), a river silts and clays

or closed basin group (CGA9 and possibly CGA1), which has some overlap with the dune group (CGA2, CGA3, CGA10 CGA12 and possibly CGA1), and a group which falls outside the parameters of the segments (CGA7, CGA8 and CGA11).

The sediments of core CGB separate into four groups: a sandy river group (CGB1, CGB5, CGB6, CGB7, CGB11 and CGB12), a river silts and clays or closed basin group (CGB3, probably also CGB8, CGB9 and CGB10), which has some overlap with the dune group (CGB2 and CGB4) and CGB13 which plots outside the parameters of the segments, but probably constitutes part of the sandy river group.

The sediments of core NR separate into four groups: a dune group (NR18 and NR25), a river silts and clays or closed basin group (NR1, NR10, NR11, NR12 and NR26), which overlaps the dune segment so could have been deposited in either environment; a group that plots outside the parameters of the segments (NR17, NR19, NR20, NR22 and NR24); the remaining units plot in the sandy river group.

Core CM sediments separate into five groups: a sandy river group (CM6, CM10, CM11 and CM12), a river silts and clays or closed basin group (CM1 and CM13), which has some overlap with the dune or river silts group (CM3), the dune group (CM2, CM4 and CM5), and CM7, CM8 and CM9 which plot outside the parameters of the segments.

Table 7.5: Summary of depositional environments indicated by segment analysis.

Units not shown plot outside the environmental parameters

Depositional environment	Units
Sandy river	GV10, possibly GV4 & GV5, PG7, possibly PG8, PGA1, PGA2, PGA14, probably PGA3 & PGA8, CGA4, CGA5, CGA, CGA13, CGB1, CGB5, CGB6, CGB7, CGB11, CGB12, NR2, NR3, NR4, NR5, NR6, NR7, NR8, NR9, NR13, NR14, NR15, NR16, NR21, NR23, CM6, CM10, CM11, CM12, TG8, TG9, TG12
River silts & clays or closed basin	GV7, possibly GV6 & GV9, PGA4, PGA5, PGA6, PGA10, CGA9, possibly CGA1, CGB3, probably CGB8, CGB9 & CGB10, NR1, NR10, NR11, NR12, NR26, CM1, CM13, possibly CM3, TG1, TG4, TG5, TG6, TG7, TG10, TG11, TG16, TG17, TG18, TG19, TG21, TG22
Dune	PG1, PG4, PGA7, CGA2, CGA3, CGA10, CGA12, possibly CGA1, CGB2, CGB4, NR18, NR25, CM2, CM4, CM5
Beach	PGA15, PGA16, PGA17, CGA14

The sediments of core TG separate into four groups: a sandy river group (TG8, TG9 and TG12); TG20 plots in the overlap between the river silts and clays or closed basin segment and the dune segments; TG2, TG3, TG13, TG14 and TG15 plot outside the parameters of the segments. The remainder and largest group of units plot in the river silts and clays or closed basin group.

7.3 Bivariate plots of gravel clast morphology

Bivariance of limestone gravel clast morphology parameters (mean sphericity against mean OPI) was used to differentiate river and beach depositional characteristics and bivariance of clast morphology against roundness (C_{40} against RA) was used to determine whether any of the gravels had glacial characteristics.

7.3.1 Bivariance of gravel clast sphericity and OPI

The bivariate plot of mean clast sphericity against mean OPI (Figure 7.7) indicates beach depositional characteristics for most of the Gordano Valley gravels; fluvial characteristics are indicated for PG7, CGB1, CGB7, NR9, NR13, NR21 and TG3.

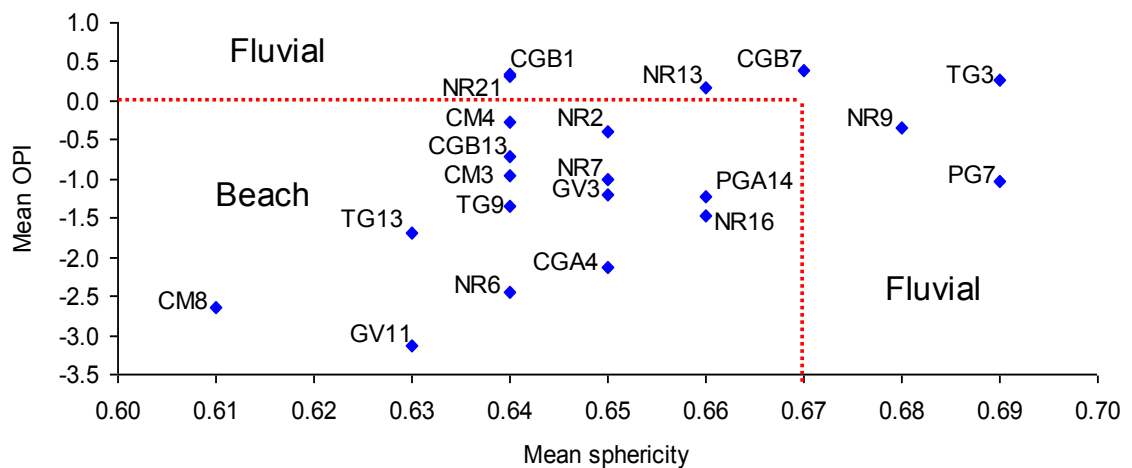


Figure 7.7: Bivariate plot of mean sphericity against mean OPI (adapted from Dobkins & Folk 1970) for Gordano Valley gravels. The plots for CGB1 and NR21 coincide. The dotted red line represents the boundary between beach and fluvial environments

7.3.2 Bivariance of gravel clast morphology and roundness

The bivariate plot of clast morphology against roundness (Figure 7.8) indicates moraine characteristics for most of the Gordano Valley gravels, with a number of gravels also plotting marginally to the moraine envelope. NR21 plots close to the envelope for deposits of known scree origin.

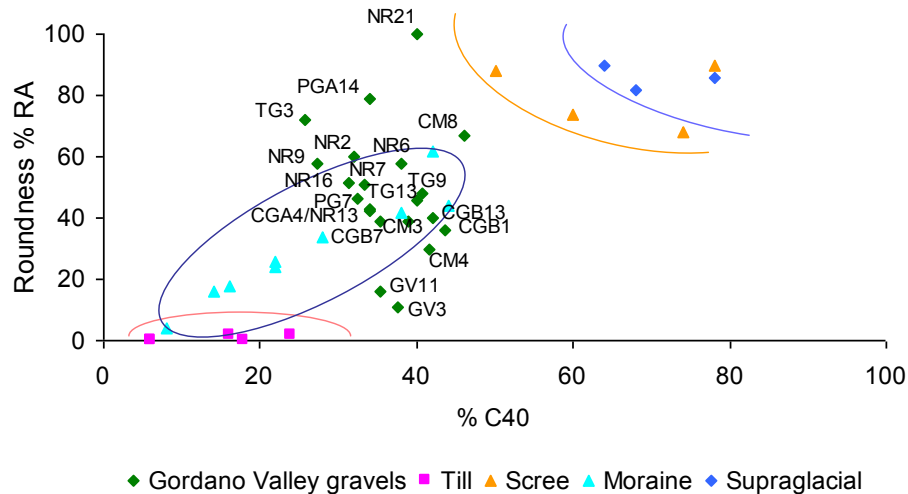


Figure 7.8: Bivariate plot of %C₄₀ against %RA (adapted from Evans & Benn 2004 with additional data from Benn & Ballantyne 1993, 1994). Most gravels plot within the parameters for known moraine deposits; CGA4 and NR13 coincide on the plot. CGB1, NR2, NR9 and CM4 plot marginally to deposits of known moraine origin and NR21 plots close to deposits of known scree origin

7.3.3 Gravel clast morphology histograms

Frequency histograms of the values of gravel clast (a-b)/(a-c) measurements (Sneed & Folk 1958) are shown in Figure 7.9. Polymodal distributions for most Gordano Valley gravels indicate the gravels comprise multiple components. However, CM4 and CM8 have bimodal distributions, suggesting these gravels comprise just two components, whilst GV3 has an almost Gaussian distribution, indicating this gravel does not comprise multiple components.

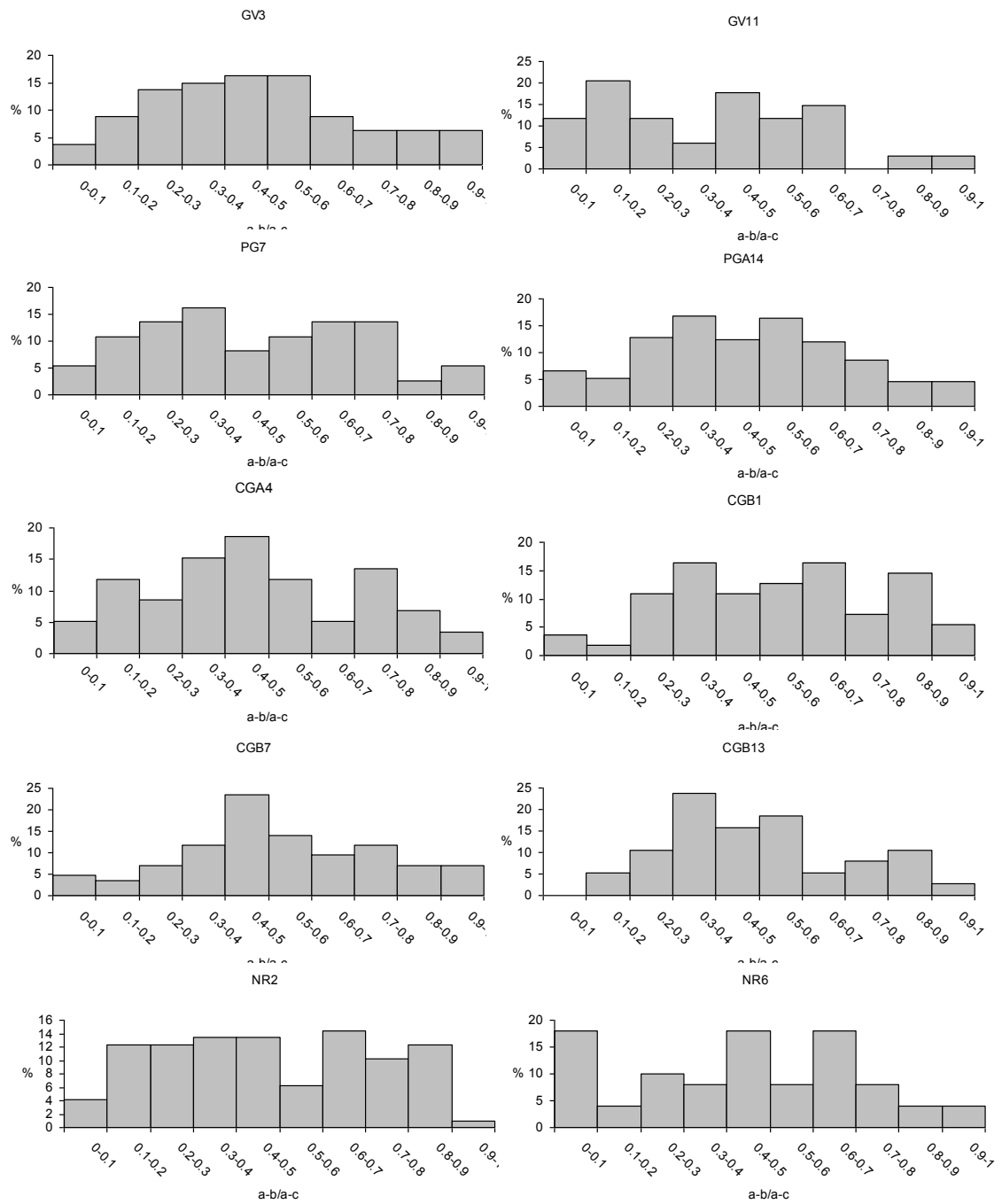


Figure 7.9: Frequency histograms of the values of the $(a-b)/(a-c)$ measurements for the Gordano Valley gravels (adapted from Sneed & Folk 1958)

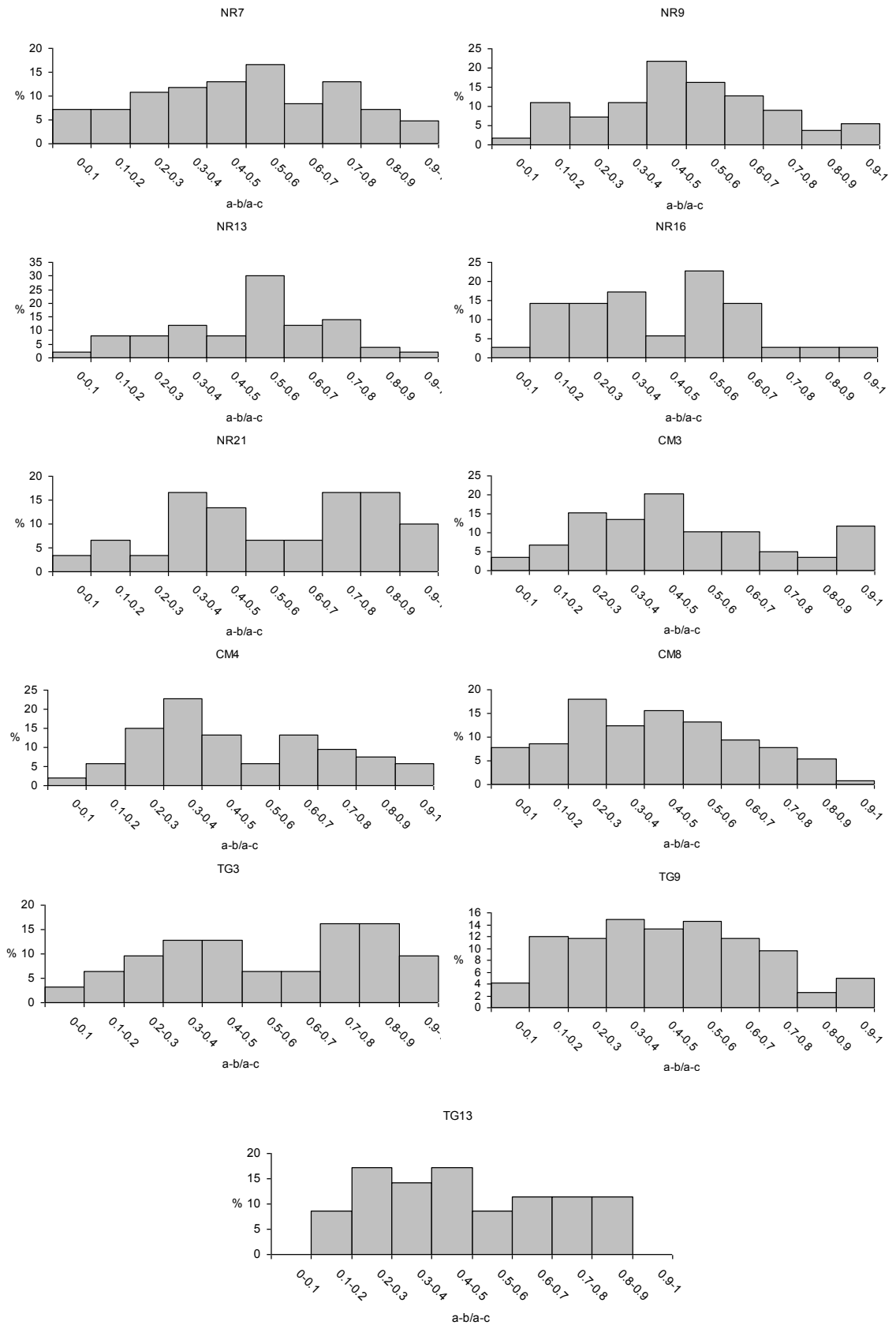


Figure 7.9 (continued): Frequency histograms of the values of the $(a-b)/(a-c)$ measurements for the Gordano Valley gravels (adapted from Sneed & Folk 1958)

7.4 Interpretation of sedimentary evidence of depositional environments

The sedimentary attributes inferred from the analyses presented above, together with the results for clast lithological analysis presented in section 6.4, allow an interpretation of the depositional characteristics to be made for each sedimentary unit. Characteristics inferred from particle size attributes are assessed first, followed by those from gravel clast morphology and roundness.

7.4.1 General sedimentary characteristics

Most units have bi- or multimodal particle size distributions, indicative of reworked deposits (Weltje & Prins 2007); there are no unimodal particle size distributions in cores PG, CGB and CM and most units are very to extremely poorly sorted. Table 7.6 shows that all units have some characteristics of settling deposition (indicative of closed basin deposition: lake, lagoon, estuary, delta, floodplain or tidal flat for example, Tanner 1991), which probably reflects the configuration of the valley. Fluvial characteristics are also indicated for most units: only seven units show no characteristics of fluvial deposition. Sixty seven units have some characteristics of aeolian deposition, twenty units have the characteristics of deposition from mudflow and forty one units have some characteristics of beach deposition. Sediment sorting indicates beach deposition is likely, therefore where beach characteristics are indicated these are attributed to winnowing of fine material under waning flow and sediments are interpreted as fluvial lag deposits.

Analysis of gravel attributes (Table 7.7) indicates that gravel units were deposited in either fluvial or beach environments. Fluvial characteristics are indicated for eight gravels, whilst high energy beach characteristics are indicated for two gravels (GV11 and CM8), low energy beach characteristics are indicated for ten gravels and NR6 is shown to be both a high and low energy beach; only NR16 is indeterminate, being either fluvial or beach gravel. Fourteen gravel units (PG7, CGA4, all core CGB and CM gravels, four gravels in core NR and two gravels in core TG) have characteristics of glacial (moraine) deposition and NR21 has scree characteristics.

Table 7.6: Summary of depositional characteristics from particle size evidence

Unit	GV1	GV2	GV3	GV4	GV5	GV6	GV7	GV8	GV9	GV10	GV11
Segment	*	*	*	R	R	D/R/S	R/S	*	R/S	R	*
sk v k	B	S	D/S	D/S	D/S	R	R	R	R	R	D/S
>4 ϕ x v σ	R	R	S	S	R	S	S	R	S	S	S
Median v sk	*	*	*	*	*	*	*	*	R	R	*
Median v σ	S	S	*	*	*	*	S	S	*	*	*
Median v coarsest 1 %	M	M	*	*	*	R	R	M	R	R	*
Unit	PG1	PG2	PG3	PG4	PG5	PG6	PG7	PG8			
Segment	D	*	*	D	*	*	R	*			
sk v k	B	R	R	R	R	R	D/S	R			
>4 ϕ x v σ	S	S	S	S	S	S	S	S			
Median v sk	B	*	*	R	*	*	R	R			
Median v σ	*	S	S	*	S	S	*	*			
Median v coarsest 1 %	R	M	M	R	*	*	R	R			
Unit	PGA1	PGA2	PGA3	PGA4	PGA5	PGA6	PGA7	PGA8	PGA9	PGA10	PGA11
Segment	R	R	*	R	R	R	D	*	*	R	*
sk v k	S	S	S	S	R	B	R	S	R	R	R
>4 ϕ x v σ	S	S	S	S	S	S	S	S	S	S	S
Median v sk	R	*	R	*	*	*	B	*	B	*	*
Median v σ	*	*	*	*	*	S	*	*	S	S	S
Median v coarsest 1 %	R	R	R	R	M	R	R	R	I	M	M
Abbreviations:	B = beach; D = dune/aeolian; R = river; S = settling; M = mudflow, I = intermediate (between mudflow and river)										
	* = plots outside parameters of environmental envelopes										
	Settling = closed basin, lagoon, estuary, lake, delta, floodplain, tidal flat										

Table 7.6 (continued): Summary of depositional characteristics from particle size evidence

Unit	PGA12	PGA13	PGA14	PGA15	PGA16	PGA17								
Segment	*	*	R	B	B	B								
sk v k	B	R	R	S	S	S								
>4 φ x v σ	S	S	S	S	S	S								
Median v sk	*	*	R	*	*	*								
Median v σ	S	S	*	*	*	*								
Median v coarsest 1 %	M	M	R	R	R	R								
Unit	CGA1	CGA2	CGA3	CGA4	CGA5	CGA6	CGA7	CGA8	CGA9	CGA10	CGA11	CGA12	CGA13	CGA14
Segment	R/D	D	D	R	R	R	*	*	R	D	*	D	R	B
sk v k	B	R	D/S	D/S	D/S	D/S	R	R	B	D/S	B	B	B	D/S
>4 φ x v σ	S	S	S	S	S	S	S	S	S	S	S	S	S	S
Median v sk	B	B	B	*	R	R	B	*	*	B	B	B	R	*
Median v σ	*	S	*	*	*	*	S	S	S	*	S	*	*	R
Median v coarsest 1 %	R	I	R	*	R	R	*	I	M	R	I	R	R	*
Unit	CGB1	CGB2	CGB3	CGB4	CGB5	CGB6	CGB7	CGB8	CGB9	CGB10	CGB11	CGB12	CGB13	
Segment	R	D	R	D	R	R	R	D/R	D/R	D/R	R	R	*	
sk v k	D/S	D/S	D/S	D/S	D/S	D/S	D/S	B	D/S	B	B	B	D/S	
>4 φ x v σ	S	S	S	S	S	S	S	S	S	S	S	S	S	
Median v sk	*	*	R	S	S	*	*	B	R	B	B	B	R	
Median v σ	*	*	*	S	*	*	*	*	*	*	S	*	*	
Median v coarsest 1 %	R	R	R	R	R	R	R	R	R	R	*	*	R	
Abbreviations:	B = beach; D = dune/aeolian; R = river; S = settling; M = mudflow, I = intermediate (between mudflow and river)													
	* = plots outside parameters of environmental envelopes													
	Settling = closed basin, lagoon, estuary, lake, delta, floodplain, tidal flat													

Table 7.6 (continued): Summary of depositional characteristics from particle size evidence

Unit	NR1	NR2	NR3	NR4	NR5	NR6	NR7	NR8	NR9	NR10	NR11	NR12	NR13
Segment	D/R/S	R	R	R	R	R	R	R	R	D/R/S	D/R/S	D/R/S	R
sk v k	D/S	D/S	B	D/S	D/S	D/S	D/S	B	D/S	D/S	D/S	D/S	D/S
>4 ϕ x v σ	S	S	S	S	S	S	S	S	S	R	S	S	S
Median v sk	*	*	R	*	R	*	R	R	*	S	S	R	R
Median v σ	*	*	*	*	*	*	*	*	*	*	*	*	*
Median v coarsest 1 %	R	*	R	R	R	R	R	R	*	R	R	R	R
Unit	NR14	NR15	NR16	NR17	NR18	NR19	NR20	NR21	NR22	NR23	NR24	NR25	NR26
Segment	R	R	R	*	D	*	*	R	*	R	*	D	D/R/S
sk v k	D/S	D/S	D/S	R	R	D/S	R	D/S	R	B	D/S	B	D/S
>4 ϕ x v σ	S	S	R	S	S	R	S	S	S	R	S	S	S
Median v sk	*	*	*	B	B	R	*	R	B	R/B	R	B	S
Median v σ	*	*	*	*	*	*	S	*	S	*	*	*	*
Median v coarsest 1 %	R	*	*	R	R	R	M	R	*	R	R	R	R
Unit	CM1	CM2	CM3	CM4	CM5	CM6	CM7	CM8	CM9	CM10	CM11	CM12	CM13
Segment	R	D	D/R	D	D	R	*	*	*	R	R	R	R
sk v k	R	D/S	D/S	D/S	R	R	R	D/S	R	B	D/S	B	B
>4 ϕ x v σ	S	S	S	S	S	S	S	S	S	S	S	S	S
Median v sk	*	R	*	R	*	*	*	R	R/B	B	S	B	*
Median v σ	S	*	*	*	S	S	S	*	*	*	*	*	S
Median v coarsest 1 %	M	R	R	R	M	M	M	R	R	R	R	*	R
Abbreviations:	B = beach; D = dune/aeolian; R = river; S = settling; M = mudflow, I = intermediate (between mudflow and river)												
	* = plots outside parameters of environmental envelopes												
	Settling = closed basin, lagoon, estuary, lake, delta, floodplain, tidal flat												

Table 7.6 (continued): Summary of depositional characteristics from particle size evidence

Unit	TG1	TG2	TG3	TG4	TG5	TG6	TG7	TG8	TG9	TG10	TG11
Segment	R	*	*	R	R	R	R	R	R	R	R
sk v k	R	D/S	D/S	D/S	D/S	B	B	D/S	D/S	R	B
>4 ϕ x v σ	S	S	S	S	S	S	S	S	S	S	R
Median v sk	*	*	*	*	*	*	*	R	*	*	*
Median v σ	*	*	*	S	*	*	*	*	*	S	S
Median v coarsest 1 %	M	*	*	R	R	R	R	R	R	M	M
Unit	TG12	TG13	TG14	TG15	TG16	TG17	TG18	TG19	TG20	TG21	TG22
Segment	R	*	*	*	R	R	R	R	D/R	R	R
sk v k	D/S	D/S	D/S	R	B	D/S	B	D/S	B	D/S	B
>4 ϕ x v σ	S	S	S	S	S	S	S	S	S	S	S
Median v sk	R	*	*	*	*	*	*	*	B	*	*
Median v σ	*	*	*	S	*	*	S	*	S	S	*
Median v coarsest 1 %	R	R	*	M	R	R	R	R	R	R	R
Abbreviations:	B = beach; D = dune/aeolian; R = river; S = settling; M = mudflow, I = intermediate (between mudflow and river)										
	* = plots outside parameters of environmental envelopes										
	Settling = closed basin, lagoon, estuary, lake, delta, floodplain, tidal flat										

Table 7.7: Summary of depositional characteristics from clast morphology and roundness

Unit	GV3	GV11	PG7	PGA14	CGA4	CGB1	CGB7	CGB13	NR2	NR6	NR7
Morphology	B/R	B	R	R/B							
Mean OPI	B(LE)	B(HE)	B(LE)	B(LE)	B(LE)	R	R	B(LE)	B(LE)	B(LE)	B(LE)
Mean sphericity	B	B	R	B	B(LE)	B	R	B	B(LE)	B(HE)	B
Roundness	B/R	R	R	R	R	R	R	R	R	R	R
%C ₄₀ v %RA	*	*	Q	*	Q	Q	Q	Q	*	Q	Q
Mean sphericity v mean OPI	B	B	R	B	B	R	R	B	B	B	B
Unit	NR9	NR13	NR16	NR21	CM3	CM4	CM8	TG3	TG9	TG13	
Morphology	R/B	R/B	R/B	R	R/B	R/B	R/B	R	R/B	R	
Mean OPI	B(LE)	R	B(LE)	R	B(LE)	B(LE)	B(HE)	R	B(LE)	B(LE)	
Mean sphericity	R	B	R	B	B	B	B	R	B	B	
Roundness	R	R	R	R	R	R	R	R	R	R	
%C ₄₀ v %RA	*	Q	Q	X	Q	*	*	*	Q	Q	
Mean sphericity v mean OPI	R	R	B	R	B	B	B	R	B	B	
Abbreviations:	B = beach; (HE) = high energy beach; (LE) = low energy beach;										
	R = river; X = scree; Q = moraine; * = plots outside parameters of environmental envelopes										

Reworking is also evident for gravel clasts in most units, indicated by their polymodal shape distribution (Figure 7.9), suggesting multiple components, except possibly not for GV3 which has a unimodal distribution. The presence of broken clasts together with a wide variation in clast shape for CGA4, CGB1, NR6, NR7, NR9, NR13, NR16, NR21, CM3, CM4, CM8, TG3, TG9 and TG13 indicates high-energy transportational conditions (Dobkins & Folk 1970, Hart 1991) and reworking.

7.4.2 Sedimentary evidence

A depositional environment for each unit was inferred by following the procedure outlined in section 4.12.1. Combining the two sets of data allowed additional evidence to be brought to bear on gravel units. For units GV3 and GV11 this resulted in an indeterminate depositional environment, and an attempt has been made to accommodate all possibilities in their interpretation. Although GV1 has the characteristics of deposition from a muddy river it was identified as Triassic mudstone bedrock (S.B. Marriott, 2005, Pers. comm.). Inferred depositional environments are summarised in Table 7.8.

Only PGA12 has characteristics of deposition from mudflow. GV2, GV8, PG2, PG3, PGA5, PGA9, PGA10, PGA11, PGA13, CGA2, CGA7, CGA8, CGA9, CGA11, NR20, CM1, CM5, CM6, CM7, TG1, TG10, TG11 and TG15 all demonstrate both fluvial and mudflow characteristics consistent with deposition from a muddy river whilst PG5, PG6 and NR22 demonstrate fluvial characteristics and probable mudflow characteristics and are also interpreted as muddy river deposits. CGA2 has characteristics of a fluvial and mudflow lag deposit; it contains small-scale rippled laminations (Figure 6.3D), indicative of deposition under flowing water (Reineck & Singh 1973). Similar small-scale ripples are described by Marriott (1996) in flood deposits on the bank of the River Severn. The laminated/thin bedding of TG10 also indicates deposition under flowing water (Evans & Benn 2004). Additional beach characteristics for CGA7, CGA11 and TG11 suggest these were probably deposited under waning flow conditions. Additional aeolian characteristics in CGA2 and CM5 indicate reworking of pre-existing aeolian deposits.

GV6, GV7, PGA4, PGA6, PGA8, PGA15 to PGA17, CGA1, CGA14, CGB5, CGB6, CM11, CM13, NR11, TG4 to TG7 and TG16 to TG22 demonstrate the characteristics of deposition in a braided stream. Additional characteristics of aeolian deposition for GV6, CGA1, CGA14, CGB5, CGB6, CM11, NR11, TG4, TG5, TG17,

TG19, TG20 and TG21 indicate reworking of pre-existing aeolian material, whilst CGA1, CGA14, CM13, TG6, TG7, TG16, TG18, TG20 and TG22 have characteristics of braided stream lag deposits. CGB11 and CGB12 demonstrate characteristics which may be those of braided stream or, more probably, river channel lag deposits.

Table 7.8: Summary of inferred depositional environments

Inferred depositional environment	Units
Aeolian	CGA3, CGA10, CGB4, NR1, NR10, NR26, CM2
Mudflow	PGA12
Muddy river	GV2, GV8, PG2, PG3, PG5, PG6, PGA5, PGA9, PGA10, PGA11, PGA13, CGA8, CGA9, NR20, NR22, CM1, CM5, CM6, TG1, TG10, TG15
Muddy river lag deposit	CGA2, CGA7, CGA11
Braided stream	GV6, GV7, PGA4, PGA6, PGA8, PGA15, PGA16, PGA17, CGB5, CGB6, CM11, NR11, TG4, TG5, TG17, TG19, TG21
Braided stream lag deposit	CGA1, CGA14, CM13, TG6, TG7, TG16, TG18, TG20, TG22
Turbulent sand-bedded river channel	PG1
Sand-bedded river channel	GV9, GV10, PG4, PG8, PGA1, PGA7, CGA5, CGA6, CGA12, CGA13, CGB3, NR13
Silt/sand-bedded river channel lag deposit	CGB8, CGB10, CGB11, CGB12, NR3, NR8, NR23, NR25, CM9, CM10, CM12, TG8, TG12
Turbulent gravel-bedded river channel	GV4, GV5, TG2, TG3
Turbulent gravel-bedded river channel lag deposit	GV3, GV11
Turbulent gravel-bedded river	NR4, TG14
Turbulent gravel-bedded river lag deposit	CGA4, CGB13, NR16
High-energy gravel-bedded river channel	NR2, NR5, NR13
High-energy gravel-bedded river lag deposit	PG7, PGA14, CGB7, NR6, NR7, NR9, NR21, CM3, CM4, CM8, TG9, TG13
Gravel-bedded river channel	PGA2, PGA3, CGB9, NR19, NR24
Gravel-bedded river	CGB2, NR14
Gravel-bedded river lag deposit	CGB1, NR15, NR17

GV9, GV10, PG4, PG8, PGA1, PGA7, CGA5, CGA6, CGA12, CGA13, CGB3, CGB8, CGB10, NR3, NR8, NR12, NR18, NR23, NR24, NR25, CM9, CM10, CM12, TG8 and TG12 demonstrate the characteristics of river channel deposits. Additional aeolian characteristics for PG4, PGA7, CGA5, CGA6, CGA12, CGB3, CGB8, CGB10, NR3, NR12, NR18, NR24, NR25, TG8 and TG12 indicate the presence of reworked aeolian material, whilst CGB8, CGB10, NR3, NR8, NR18, NR23, NR25, CM9, CM10, CM12, TG8 and TG12 display additional characteristics which indicate these are lag deposits.

CGB4, NR1, NR10 and NR26 demonstrate the characteristics of aeolian and braided stream deposition suggesting possible deflation of local fluvial deposits and accumulation in a sheltered topographic hollow. CGA3, CGA10 and CM2 have characteristics of river channel and aeolian deposition, also probably from deflation and reworking of local fluvial deposits by wind. CGA3 and CGA10 demonstrate additional characteristics of fluvial lag deposits.

GV4, GV5, PGA2, PGA3, CGB9, NR2, NR5, NR13, NR14, NR19 and TG3 demonstrate the characteristics of deposition in the channel of a gravel-bedded river, whilst GV3, GV11, PG7, PGA14, CGA4, CGB1, CGB7, CGB13, NR6, NR7, NR9, NR15, NR16, NR17, NR21, CM3, CM4, CM8, TG9 and TG13 have the characteristics of lag deposits in the channel of a gravel-bedded river. The presence in CM3 and TG9 of imbricated gravel clasts indicates water-lain deposition, and supports their interpretation as fluvial deposits, whilst the presence of broken clasts and the wide variation in clast shape in PG7, PGA14, CGB7, NR2, NR5, NR6 and NR7 indicates high-energy transportational conditions (Dobkins & Folk 1970, Hart 1991); GV3, GV4, GV5, GV11, CGA4, NR16 and TG3 demonstrate characteristics of deposition from turbulent flow, and possible rip-up clasts in TG9, incorporated from bed or bank material, also indicate turbulent flow (Evans & Benn 2004). Additional aeolian characteristics in GV3, GV11, CGB9, NR2, NR5, NR9, NR14, NR15, NR19, NR21, CM4, CM8 and TG3, and aeolian and moraine characteristics in PG7, CGA4, CGB1, CGB7, CGB13, NR6, NR7, NR13, NR16, CM3, TG9 and TG13 indicate reworking of pre-existing deposits.

Although the characteristics of CGB2, NR4, TG2 and TG14 indicate river channel and aeolian deposition, suggesting possible deflation of local fluvial deposits, particle size analysis indicates that CGB2, NR4, TG2 and TG14 are gravel units. They are more probably fluvial deposits; this is supported by limited evidence from gravel clast morphology which also indicates a fluvial depositional environment, possibly channel lag

in a gravel-bedded river. The characteristics of PG1 also indicate river channel and aeolian deposition, suggesting possible deflation of local fluvial deposits. However, the silt inclusion in PG1 (Figure 6.1D) is probably a rip-up clast (Evans & Benn 2004) incorporated from bed or bank material, supporting a fluvial interpretation. Possible rip-up clasts are also present in TG2, suggesting turbulent flow. Evidence suggests that NR4 and TG14 were probably deposited under turbulent flow conditions; their aeolian characteristics probably represent reworked aeolian material and the incorporation of pre-existing aeolian deposits into the gravel matrix.

7.5 Gravel provenance

The gravel clasts of GV3, GV11, CGA4, CGB1, CGB7, NR2, NR6, NR7, NR9, NR13, NR16, NR21, CM3, CM4, CM8, TG3, TG9 and TG13 are predominantly limestone and probably represent an input from a local source. A brown sandstone component in most of these gravels is probably also locally derived, either from the Devonian outcrop on the Clevedon-Portishead ridge and/or locally available glacial deposits from the Clevedon-Portishead or Tickenham ridges (Hawkins 1972, Gilbertson & Hawkins 1978a, Hunt 2006e). A quartz and/or quartzite component in many of the gravels may derive from further afield or represent reworking of earlier deposits. For example, angular and sub-round quartz and quartzite clasts of CGB7 may indicate locally derived clasts mixed with those that have been undergoing transport for a long time, suggesting that material has been recycled.

Clast morphological analysis indicates CGB1, CGB7, CGB13, NR6, NR13, NR16, CM3, TG9 and TG13 are partly composed of reworked moraine deposits, which suggests remobilisation of glacial deposits either from Nightingale Valley or Court Hill (Gilbertson & Hawkins 1978a, Hunt 2006e). This is supported by the presence of a minor flint component in GV3, CGA4, CGB7, NR7, NR13, NR16, CM3, CM4, CM8 and TG3, and an exotic component in NR6 (ironpan) and NR9 (iron pan, flint, granite and possibly tourmaline). The ironpan clast in NR6 has a lot of sand as host sediment, which would be exotic to Tickenham Ridge, the nearest source for gravel clasts. The presence of broken clasts which demonstrate secondary edge-rounding in GV3 could be the result of glacial abrasion if the clasts are derived from till (Harris 1987); alternatively it may be due to subsequent reworking in a water-lain environment.

The limestone gravel clasts of CGB1, CM3, CM4 and TG9 are angular to sub-round indicating a certain amount of transport, whereas the predominantly angular to sub-angular limestone clasts of GV3, GV11, CGA4, CGB7, NR6, NR7, NR9, NR13, NR16, CM8 and TG13 indicate a short duration of transport, probably less than 8 to 16 km (Wentworth 1922, Sneed & Folk 1958) and local provenance. The very angular to angular limestone gravel clasts of TG3 and the very angular clasts of NR2 and NR21 indicate an extremely short duration of transport (Wentworth 1922); the clast morphology of NR21 suggests possible deposition as scree.

From the limited evidence available, the gravel clasts in GV4, GV5, PGA2, PGA3, CGB2, NR4, NR14, NR15, NR17, NR19, NR24 and TG2 also appear to be predominantly limestone from a local source. There is a contribution from non-limestone lithologies which in GV4 and NR14 is entirely brown sandstone, probably either from the Devonian outcrop on the Clevedon-Portishead ridge or from the glacial deposits of the Clevedon-Portishead and Tickenham ridges (Hawkins 1972, Gilbertson & Hawkins 1978a, Hunt 2006e), and in NR4, NR15, NR17 and NR19 entirely comprises locally available lithologies. The presence of angular or sub-round quartz and quartzite clasts in PGA3, and the flint component of PGA3 and CGB2 suggest inputs from glacial deposits, probably of Nightingale Valley (Hunt 2006e), together with a mixture of recycled material. Additionally, their very angular to sub-angular limestone clasts indicate a short to extremely short duration of transport, probably less than 8 to 16 km (Wentworth 1922, Sneed & Folk 1958).

GV5 has a relatively large quartz and quartzite component, which may be derived from further afield, although the durability of these rocks may indicate a long transport history prior to their incorporation into the gravel of GV5 or their relative abundance may be the result of the greater susceptibility of limestone to weathering which has left the gravel relatively enriched in the more durable lithologies (Evans & Benn 2004). The sub-round and round limestone clasts of GV5 suggest long or repeated periods of water transport (Mills 1979).

PG7, PGA14, and CGB13 are predominantly brown sandstone and probably represent inputs from a local source such as the Devonian outcrop on the Clevedon-Portishead ridge or from the glacial deposits of Nightingale Valley (Hunt 2006e). The latter possibility is strengthened for PG7 and CGB13 by analysis indicating previous deposition as a moraine and by the presence of flint and in PG7 of granite and Triassic sandstone clasts. Triassic sandstone is reported among the exotic clasts of Nightingale Valley and

Court Hill glacial deposits (Gilbertson & Hawkins 1978a, Hunt 2006e). The limestone gravel clasts of PG7 and PGA14 are predominantly angular indicating extremely short duration of transport (Wentworth 1922) and probable local provenance. However, the limestone gravel clasts of CGB13 are predominantly sub-angular, indicating they have undergone a certain amount of transport (Wentworth 1922).

Although evidence is limited, the gravel component of GV2, PG6 and CGB9 appears to be dominated by brown sandstone, either from the Devonian outcrop on the Clevedon-Portishead ridge or from the glacial deposits of Nightingale Valley or Court Hill (Gilbertson & Hawkins 1978a, Hunt 2006e). In GV2 the brown sandstone clasts have been compressed into what may be weathered bedrock. Here, the apparent dominance of brown sandstone over limestone could indicate the relative enrichment of the gravel with a more durable lithology due the greater susceptibility of limestone to weathering (Evans & Benn 2004). The gravel clasts of GV2 are completely or highly weathered, which suggests long or repeated periods of surface exposure. Limestone gravel clasts of GV2 and PG6 are sub-round, suggesting long or repeated periods of water transport or rounding prior to their latest transportation (Mills 1979). CGB9 appears to mark a local change in gravel source, from predominantly limestone in the underlying gravels to predominantly brown sandstone in those overlying the unit. The limestone gravel clasts of this unit are predominantly sub-angular, indicating they have undergone a certain amount of transport (Wentworth 1922).

7.6 Palaeontology

The fragmentary nature of many of the fossil remains indicates reworking of sediment and/or high energy depositional environments, and the shell fragments and detrital organic remains found in many units suggest inwashed material, again indicating reworking of sediment.

7.6.1 Pollen evidence

Pollen records in fluvial environments tend to be fragmentary (Keen 2001) and low concentrations, as exhibited by the sediments of core GV, are not uncommon in a fluvial environment (Brown 1996). The pollen recovered from GV7, GV8 and GV9 is indicative

of a damp, disturbed ground, near freshwater (McClintock & Fitter 1956). Given the rarity of the pollen grains it is likely they are inwashed from local but earlier deposits.

7.6.2 Plant macrofossil evidence

The derived wood fragment in PG3 indicates trees and/or shrubs growing nearby prior to deposition of PG3 and was probably brought in by flood water. The abrupt start and termination of vertically oriented reed stems in CM6 suggests high energy transportation in reworked sediment, and that their orientation is random. In contrast, the vertical orientation of plant stems in CM5 and CM13 indicates *in situ* growth, pedogenesis and landscape stability (Tucker 2003), whilst *in situ* reed stems and organic material found in the upper units of core NR (NR16 or above) indicate vegetation growth prior to burial. The reed stems in NR25, NR23, NR21, NR19 and NR17 suggest nearby shallow fresh or brackish water (McClintock & Fitter 1956). The green reed stem in NR25 suggests the presence of chlorophyll, photosynthesis and recent burial, although the depth of burial (2.54 m) would seem to preclude this possibility. This suggests possible disturbance of the surface and uppermost units of core NR.

7.6.3 Mollusc evidence

The presence of molluscs in the gravels of core GV indicates that vegetation was locally present. If the shell in GV3 is *Belgrandia marginata*, then this is a thermophilous species at present found only in small springs and streams in southern France and Catalonia, Spain, and has been identified as an important indicator of interglacial climates (Keen 2001). However, given its poor preservation state, the shell is probably derived from reworked earlier material. The *Viviparus diluvianus* shell in GV5 is well-preserved and indicates a lake or river environment (Fitter & Manuel 1986). Kerney (1971) reports the presence of *Viviparus diluvianus* from fluvial gravels at Swanscombe, north Kent.

Both TG7 and TG8 have a restricted molluscan fauna; terrestrial and estuarine molluscs were not recovered. This suggests that dry land was some distance away and that there was no regular inundation by the sea. Ecological interpretation follows Sparks (1964) in which four main groups are identified: catholic, moving water, ditch and slum.

7.6.3.1 TG7 mollusc evidence

TG7 contains an impoverished molluscan fauna; only 47 shells comprising seven freshwater species were recovered in total, although *Radix balthica* (= *Lymnaea peregra*) may be found in brackish waters as a freshwater immigrant (Wilbur & Yonge 1964, Ellis 1969). First, and most numerous, is the moving water group, composed of four species. The limpet *Ancylus fluviatilis* is widely distributed throughout the British Isles (Kerney 1976) and is found adhering to stones, sunken wood and the stems and leaves of water plants, typically in fast flowing streams, but occasionally on the wave zone of lakes or in standing water (Wilbur & Yonge, 1964, Ellis 1969, Beedham 1972). The presence of *Ancylus fluviatilis* is usually interpreted to indicate moderate stream flow (Coope *et al.* 1997), although low numbers have also been recorded in organic muds (Sparks 1964). *Pisidium subtruncatum* and *Pisidium nitidum* are fluvial species of *Pisidium* (Maddy *et al.* 1998). *Pisidium subtruncatum* occurs in a wide range of lowland aquatic environments, but shows a preference for flowing water. It inhabits substrates from mud to grit (Moorkens & Killeen 2009). *Pisidium nitidum* occurs mostly in slowly flowing streams and rivers, but also in lakes and ponds. It prefers a fairly sheltered environment and inhabits a wide range of substrate types, but prefers sandy sediments (Coope *et al.* 1997, Preece 1999, Moorkens & Killeen 2009). Preservation of *Pisidium nitidum* is usually poor because of its thin shell (Sparks 1964). Its presence in TG7 indicates limited post-depositional transport. *Sphaerium corneum* is found in flowing or standing water, in lowland rivers, stream, lakes, ponds, on mud to coarse sand substrates (Moorkens & Killeen 2009).

Pisidium obtusale is the only slum group species in TG7. It is a freshwater bivalve (Beedham 1972) which today lives in shallow stagnant or standing water and swampy habitats, especially ponds, but is also found in fens, marshes and bogs which are prone to desiccation and in the swamp areas of large rivers and lakes away from the main channel. It lives on silty substrates with high organic content (Moorkens & Killeen 2009).

The catholic group is composed of two species. *Radix balthica* (= *Lymnaea peregra*) is currently the commonest freshwater snail in the British Isles (Kerney 1976). It inhabits almost all types of freshwater habitat and even dry land, although it prefers slow-moving, calcareous, well-vegetated streams (Kerney 1971). It withstands a wide range of environmental conditions and is tolerant of a wide range of temperatures (Wilbur & Yonge 1964, Beedham 1972). Like *Radix balthica*, *Gyraulis laevis* is associated with plant-rich

marginal habitats and quiet water (Ellis 1969, Preece 1999) and has been recorded as indicative of muddy backwaters (Schreve *et al.* 2002).

The dominance of *Pisidium obtusale* indicates accumulation in a small stagnant pool (West *et al.* 1999), although the occurrence of *Ancylus fluviatilis*, *Pisidium nitidum*, *Pisidium subtruncatum* and *Sphaerium corneum* indicates moderate stream flow and persistent fluvial conditions, whilst the less demanding *Radix balthica* and *Gyraulis laevis* indicate slow moving water in vegetation-rich shallow margins (Keen 1987, Maddy *et al.* 1998), suggesting this is an interglacial fauna. However, low counts and generally poor preservation suggest the molluscs might have been washed into TG7 from nearby.

7.6.3.2 TG8 mollusc evidence

Mollusc shells in TG8 are abundant, yet comprise only eight freshwater species. There are three main groups: slum, moving water and catholic. The slum group is composed entirely of *Pisidium obtusale*. The catholic group is composed of *Radix balthica* and *Gyraulis laevis*, both associated with plant-rich marginal habitats and quiet water (Preece 1999). The moving water group is the most numerous and is composed of four species. *Valvata piscinalis* is a widely distributed species which favours flowing water, and occurs in rivers, streams and lakes (Ellis 1969, Beedham 1972, Preece 1999). It prefers deeper water than *Radix balthica*, living about 1.5 to 2 m below the surface (Kerney 1971). The presence of small numbers of *Ancylus fluviatilis*, *Pisidium subtruncatum* and *Sphaerium corneum*, typically found in fast flowing streams, and large numbers of *Valvata piscinalis*, suggest deposition in a river channel with relatively little aquatic vegetation, faster flow over sandy riffles and slow moving water in pools. *Pisidium obtusale*, *Radix balthica* and *Gyraulis laevis* indicate almost stagnant shallow river margins that were vegetation-rich, suggesting a fully interglacial assemblage.

7.6.4 Ostracod evidence

Both TG7 and TG8 contain a mixed assemblage of freshwater and estuarine/marine ostracods. However, the assemblages are somewhat different in their make up with only 20% non-marine species in TG8, compared to 55% in TG7. TG8 also contains considerably

fewer individuals than TG7. Four main groups are identified: freshwater, brackish-estuarine, outer-estuarine and marine and exotic.

7.6.4.1 TG7 ostracod evidence

The ostracod evidence of TG7 is dominated by freshwater species, of which *Heterocypris salina* is the most common. Only 13% are brackish-estuarine, 25% are outer-estuarine and marine and the exotic group accounts for 7% of the total number of ostracods, and is composed of cold northern and warm southern marine species, and also *Neonesidea globosa* a shelf-living species, probably brought in by tidal surges (J.E. Whittaker, 2010, Pers. comm.).

Many of the freshwater species are able to tolerate brackish water; *Heterocypris salina* prefers brackish water conditions and lives primarily in coastal pools and estuaries (Holmes *et al.* 2007, J.E. Whittaker, 2010, Pers. comm.). *Cypridopsis vidua* and *Cyclocypris ovum* are both active swimmers and indicate weedy, seasonal, quiet open water conditions (Coope *et al.* 1997, Keen *et al.* 1997, Preece *et al.* 2007), whilst *Prionocypris zenkeri* is another swimming ostracod associated with gently flowing perennial streams, often connected to springs, rich aquatic vegetation, and the presence of *Chara* (Murton *et al.* 2001, Holmes *et al.* 2009). *Candona neglecta* typically inhabits small ponds, springs and streams, burrowing into soft organic mud (Holmes *et al.* 2009) and *Ilyocypris bradyi* is a non-swimming species that inhabits slow flowing waters, springs and spring-fed ponds and is found on muddy substrates and aquatic vegetation (Griffiths & Holmes 2000, Holmes *et al.* 2009). *Potamocypris zschokkei* is associated with slow flowing springs, spring-fed ponds and streams (Murton *et al.* 2001, Holmes *et al.* 2009). *Herpetocypris reptans* inhabits sluggish streams and permanent water bodies of all sizes, and is associated with dense aquatic vegetation (Holmes *et al.* 2009).

Leptocythere psammophila is the most numerous of the brackish-estuarine group and inhabits sandy estuarine substrates (Athersuch *et al.* 1989). The most numerous of the outer-estuarine and marine group comprises *Paradoxostoma/Sclerochilus* spp. These have not been differentiated, but are both sub-littoral inhabitants, living on algae. They are also known from brackish water and intertidal algae (Athersuch *et al.* 1989). The exotic group contains cold indicators (for example, *Hemicytherura clathrata*, *Finmarchinella angulata*)

and warm indicators (for example, *Aurila convexa*) that would not live in the Severn Estuary area today.

The dominant freshwater species in TG7 are best explained as *in situ*, living in estuary-marginal freshwater pools and shallow streams with perennial flow, rich in aquatic vegetation. TG7 was probably at the limit of tidal influence, subject to occasional marine inundation which transported the marine and exotic species inland from the marine shelf. The estuarine, marine and exotic species were incorporated into the sediment at times of high tide and wash-overs. Alternatively, the estuarine, marine and exotic components may have been reworked from an earlier deposit.

7.6.4.2 TG8 ostracod evidence

In contrast to TG7, the ostracod evidence of TG8 is dominated by outer-estuarine and marine species, of which *Hemicythere villosa* and *Hirschmannia viridis* are the most common. Only 20% are freshwater, 9% are brackish-estuarine and 22% are outer-estuarine and marine. The exotic group accounts for 24% of the total number of ostracods, and is mainly composed of cold northern marine species with some warm southern marine species.

Candona neglecta, the most numerous of the freshwater species, is known to tolerate slightly brackish coastal waters (Bates *et al.* 2002), whilst the brackish-estuarine component is entirely *Leptocythere psammophila* which inhabits sandy estuarine substrates (Athersuch *et al.* 1989). Of the outer-estuarine and marine species, *Leptocythere tenera*, *Palmoconcha laevata* and *Hemicythere villosa* are associated with sediment substrates in sub-littoral waters (Athersuch *et al.* 1989), although *Palmoconcha laevata* also occurs in rock pools (Athersuch *et al.* 1989). *Hemicythere villosa* is also known to inhabit littoral to shallow sub-littoral algae, whereas *Hirschmannia viridis* is exclusively phytal, occurring mainly in weed-rich littoral fringes in both marine and brackish water, and can tolerate low (2-3‰) salinity levels (Athersuch *et al.* 1989). The exotic group comprises the same cold and warm indicators as TG7.

The ostracod evidence of TG8 is best explained as living in algal-rich littoral and estuary-marginal slightly brackish pools. TG8 was probably subject to frequent marine inundation which transported the marine and exotic species inland from the marine shelf, and these were incorporated into the sediment at times of high tide. The ostracods of TG8

are a very mixed group which possibly represent reworking of earlier deposits, most likely those of TG7.

7.6.5 Foraminiferal evidence

Both TG7 and TG8 contain a mixed assemblage of intertidal and marine shelf foraminifera, with similar counts of species and total numbers. The assemblages differ slightly in their make up, mostly in the marine shelf species present. Both units are dominated by *Elphidium williamsoni*, which is an intertidal, brackish lagoon or estuarine species. Because the units have similar assemblages, they are considered together.

The most numerous species in both units are *Elphidium williamsoni*, *Cibicides lobatulus* and *Haynesina germanica*, which are all intertidal species, although *Cibicides lobatulus* is also found in estuary mouth and nearshore environments (Murray 1979). *Asterigerinata mamilla* are the most numerous of the marine shelf species, although these are overall very poorly represented. The fauna includes *Globigerina*, *Lagena* and *Oolina* species which are easily transported by currents (Kidson *et al.* 1978). This implies that the marine shelf species were transported in by the tide.

Elphidium williamsoni and *Haynesina germanica* are often found on the unvegetated seaward side of salt marsh (Alve & Murray 1999). Haslett *et al.* (1998) found that in the modern Severn Estuary *Elphidium williamsoni* and *Haynesina germanica*, in association with *Ammonia beccarii*, indicated saltpan, marsh creek or near-horizontal low marsh terrace deposition, rather than being strictly controlled by tidal levels, and occurred only on surfaces with impeded drainage. Overall, these are intertidal low marsh deposits which probably accumulated on tidal flats near a channel margin and were open to an influx of marine shelf species, which represent an eroding older deposit and reworking of the specimens.

7.6.6 Algal evidence

Chara fragments and oospores are found in both TG7 and TG8, so both units are considered together. *Chara* are macroscopic epipelagic aquatic algae present on all types of sediment (peat, silt, sand, decaying vegetation, carbonate grains, iron deposits, etc.). They grow anchored by means of branching underground rhizoids in sand and silt, and more

frequently populate calcareous waters, but this may extend to brackish waters (John *et al.* 2002); in the Baltic Sea, *Chara* dominate shallow and sheltered muddy fringes (Torn *et al.* 2010). They are often coated in calcium carbonate, which may be a factor in reducing the epiphytic flora which they support. There is evidence of vertical zonation of species and they may occur in both shallow and deep water (Round 1973). *Chara* is affected by sediment structure and chemistry, nutrient status of the water, depth and shading, water turbulence and grazing (Torn 2010). Van den Berg *et al.* (1998) found that *Chara aspera* required temperatures of 10°C or higher for the emergence of propagules and Walker *et al.* (2003) inferred a rise in water temperature, and pH no lower than 6-7, from the presence of *Chara* at Llanilid.

The *Chara* fragments and oospores therefore indicate a fresh or brackish water environment, in which temperatures reached at least 10°C. This suggests an interglacial age for TG7, although interstadial deposition is also possible; Coope *et al.* (1997) report several warm periods during MIS 3 and 4 and Walker *et al.* (2003) report Devensian (MIS 2) Lateglacial Interstadial July temperatures at Llanilid, South Wales, which were higher than present day.

7.6.7 Coleoptera evidence

The coleopteran evidence is restricted to fragmentary evidence found in TG7. *Staphylinidae* are known from every type of habitat that beetles occur in, and feed on algae, decaying vegetation and other insects. Algal-feeding species are especially conspicuous on sandy soils of beaches and stream-sides (Retallack 2001). Given the disarticulated condition of the remains, it is probable that the beetle is part of reworked material; however, sufficient remains were found to suggest that it was found very close to its original site of deposition.

7.6.8 Trace fossil evidence

The calcified burrow or root in PG1, although probably derived, is consistent with pedogenic carbonate deposition prior to the deposition (Alonso-Zarza 2003, Candy *et al.* 2006). The root traces of PGA11 and CGA11 indicate periods of sub-aerial exposure, a lower water table, vegetation growth and soil formation (Retallack 2001) and landscape

stability (Fenwick 1985). The root trace in CGA11 is deflected around a pebble which confirms it is *in situ* (Retallack 2001). Iron stains in CGB11 are due to the effects of rhizoturbation and probably represent root balls and stems rather than tapering and downward branching roots (Retallack 2001). This has resulted in preferential oxidation of sediment (Tucker 2003), indicating sub-aerial exposure, vegetation growth and soil formation and landscape stability (Fenwick 1985, Retallack 2001).

7.7 Post-depositional characteristics

In this section the data and analyses presented in sections 6.2, 6.6 and 6.7 are interpreted to allow determination of post-depositional environments to be made for each sedimentary unit. The sharp, planar and irregular boundaries between most units indicate discrete depositional events with intervening periods of non-deposition or erosion. Sharp contacts with overlying coarse sediment, for example in core PGA (Figure 6.2) between PGA1 and PGA2, PGA2 and PGA3, PGA6 and PGA7 and PGA13 and PGA14 indicate an erosional surface (Tucker 2003), whilst an irregular surface, for example of PGA4, also suggests erosion.

7.7.1 Voids, bioturbation, drab spots and haloes

Voids may have been produced as the result of sediment dewatering (Reineck & Singh 1973) or formed by the decay of entrapped vegetation or by air-entrapment at the time of deposition, a characteristic feature of alluvial fan deposits (Bull 1964, Reineck & Singh 1973). However, the pelleted wall of the sub-vertical void in CGB11 is suggestive of ichnofabric, possibly a dwelling burrow as there is no evidence of systematic working of sediment (Tucker 2003). The five voids in core CM all have smooth internal surfaces and display various combinations of proximal straight tube-shaped burrows, drab discolouration or drab haloes and shell fragments in the base. Because of their close association with burrows or shells and the presence of drab spots and haloes, the voids are also interpreted as ichnofabric, although it is impossible to assign the structures to any species. This indicates a former surface or near-surface that was subsequently buried and that the usual level of the water table was below the base of the burrows when they were constructed (Retallack 2001).

The near-vertical bioturbation traces found in CM5 and CM10 could be root traces or burrows. However, it is more likely they are burrows because, unlike root traces, the bioturbation traces in core CM are of regular width and do not taper or branch downwards. Their straight tube-shape is suggestive of *Skolithos* or *Monocraterion*. These ichnofacies are usually associated with littoral environments, although they may also be present in high-energy environments (Tucker 2003).

Localised drab spots are found at the base of the void in CM11, in CM6 and in CM5. The lower void in CM5 is surrounded by greenish grey (Gley1 6/1 5/GY) flame-shaped haloes of sub-mm thickness. Similar bluish- or greenish-grey haloes extending into a sediment matrix are a common feature of root traces (Retallack 2001). Alternatively they may be caused by burial gleization; the chemical reduction of iron hydroxides and oxides by anaerobic bacteria consuming organic matter buried with soil below or near the water table with water moving through soil and causing an irregular distribution of iron hydroxides and oxides and carbonate. A third option is that they are surface-water gley features, usually found in very clayey lowland soils with impermeable subsurface horizons, where anaerobic bacterial activity around roots, burrows and cracks in clayey, periodically waterlogged soil has caused chemical reduction at surfaces. Finally, they may be a result of bioturbation and differential colouring of a burrow and non-bioturbated sediment, resulting in an ichnofabric (Retallack 2001, Tucker 2003).

The probable explanation for drab spots in CM6 and CM11, because of the close association with burrows and shells, is that they were formed as a result of anaerobic bacterial activity consuming the former burrow occupants buried below the surface of the water table. The drab halo surrounding the lower void in CM5 is interpreted as the result of surface water gleization caused by anaerobic activity around a burrow in periodically waterlogged sediment.

7.7.2 Clast surface features

Surface cracks evident on both limestone and sandstone gravel clasts are probably caused by weathering, whilst the pitting visible on the surface of limestone clasts is probably the result of chemical weathering. This is the only clast surface feature found in TG14, but is not found in TG3.

Crescentic gouges (GV3, NR13 and CM4) are probably percussion marks attributable to high-velocity transport (Reineck & Singh 1973); similar features have been attributed to fluvial and beach origins (Gale & Hoare 1991). Other gouges seen on both limestone and sandstone clasts (GV3, GV5, CGB7, CGB13, TG3 and TG9) are almost straight and appear to be the result of animal boring, but could also be the result of glacial or high-velocity transport (Reineck & Singh 1973); the grooves in a limestone clast in NR16 are almost certainly the result of animal boring. Coincident with the occurrence of gouges are striated surfaces, almost exclusively on limestone clasts, and a chattermarked limestone clast in TG9, which indicate glacial or high-velocity transport (Reineck & Singh 1973).

The significance of polished pebble surfaces is unclear (Reineck & Singh 1973, Gale & Hoare 1991) but the polished surface of a siltstone clast of PGA2, sandstone clasts in CGB1 and CM3, and limestone clasts in NR2 and NR13 may be the result of wind action although the clasts lack ventifact morphology. Incipient desiccation cracks in the carbonate nodules of CGB7 are possibly the result of seasonal wetting and drying (Zhou & Chafetz 2009). The significance of secondary calcium carbonate deposits found on many limestone and sandstone clasts is discussed in more detail in section 7.7.3.

The widely varying degrees of weathering exhibited by the gravels clasts probably indicate recycling and mixing of clasts with fresh inputs, with varying lengths of sub-aerial exposure at some point in their history. In core NR, the more variable weathering of units above NR14 suggests longer periods of sub-aerial exposure or warmer temperatures during exposure than that experienced by the lower units. Alternatively, variation in weathering may reflect the different position of clasts in a weathering profile. The apparent inversion of the weathering profile in TG2 indicates its movement and redeposition *en masse*, probably from toppling of material from an unstable channel bank. The small number of fresh limestone and brown sandstone clasts probably represent scree, prised from nearby outcrops by frost weathering processes under a periglacial climate regime.

7.7.3 Carbonate deposits

Powdery carbonate coatings on gravel clasts can occur in both pedogenic and groundwater settings (Alonso-Zarza 2003); it is difficult to distinguish between the two

depositional types without micromorphological assessment and the two settings are not necessarily mutually exclusive (Alonso-Zarza 2003, Candy *et al.* 2006, Preece *et al.* 2007).

The coatings may have formed by direct precipitation of calcium carbonate onto the surface of the gravel clasts to form pedogenic carbonate coatings or rinds (Walker 2005). A small number of gravels display gradational boundaries and colour values which indicate pedogenesis, for example CGA4, and are occasionally overlain by units with relatively high clay content suggesting clay translocation and raising the possibility of pedogenic carbonate deposition. It is possible that subsequent pedogenesis may have eradicated evidence of a sharp upper boundary. However, most gravels have sharp upper and lower boundaries, common for groundwater carbonates (Alonso-Zarza 2003), lack horizonation and distinguishable soil profiles, vertical root traces and peds and are not overlain by translocated clays. These features, together with the occasional presence of clasts with calcium carbonate deposits on one face only, indicate that these are probably groundwater carbonates, deposited around a shallow water table in an arid to semi-arid climate with high rates of evaporation and evapotranspiration and intermittent rainfall (Alonso-Zarza 2003).

PGA5 displays soft white oval-shaped carbonate nodules with slightly irregular outlines which become increasingly numerous towards the base of the unit. The unit has sharp upper and lower boundaries, lacks horizonation and a distinguishable soil profile, vertical root traces and peds and is not overlain by translocated clays indicating that the carbonate nodules are groundwater deposits. These probably formed due to laterally moving waters around a near-surface, possibly seasonally fluctuating, water table in an arid to semi-arid climate with intermittent rainfall and high rates of evaporation and evapotranspiration, (Slate 1998, Alonso-Zarza 2003, Wright 2007) and indicate a long period of non-deposition (Tucker 2003). A large carbonate nodule in CGB11, soft white carbonate nodules in NR20, NR22, NR24 and NR25, and carbonate nodules in the upper 6 cm of TG16 all display a sharp boundary with host sediment, indicating an inorganic, groundwater origin (Retallack 2001, Alonso-Zarza 2003). The soft, chalky consistency of the nodules in NR20, NR22 and NR24 and the slightly calcareous host sediment of these units suggests carbonate leaching following their formation, which was probably in hydromorphic sediment with a shallow, fluctuating water table (Slate 1998).

In contrast, small carbonate nodules in CGB11 have diffuse boundaries with the host sediment, which suggests a biogenic origin, common for pedogenic carbonates

(Alonso-Zarza 2003). These are closely associated with patches of intense iron staining, which suggests sub-aerial exposure and proximity to the land surface. However, groundwater carbonates may also form in distal overbank or floodplain settings where weakly calcareous hydromorphic soils in a wet climate favour a near-surface fluctuating water table and alternately oxidising and reducing environments (Slate 1998); the sharp upper and lower boundaries of CGB11 also suggest groundwater formation.

Tufa clasts in PG6, PGA3, PGA14 and CM3 indicate the local presence of environments which support the formation of groundwater carbonates and erosion of a local freshwater feature that has resulted in gravel-sized clast production. Tufa occupies a variety of positions within the hydrological and geomorphological system (Viles & Pentecost 2007) and formation occurs under a range of climatic regimes from cool temperate to semi-arid, although most British tufa deposits are inferred to have been produced under warm, wet interglacial conditions (Ford & Pedley 1996). Tufa forms in calcareous, freshwater environments such as lake and pond margins, seasonal wetlands and groundwater discharge zones (spring resurgences, seepages or fast flowing calcareous streams, particularly where there are waterfalls) (Pentecost 1981, Wright & Platt 1995, Baker & Simms 1998, Freydet & Verrecchia 2002, Pedley *et al.* 2003, Verrecchia 2007, Wright 2007) or waterlogged valley-bottoms (Pedley *et al.* 2003) such as exists in the Gordano Valley today. Feasible environments for tufa formation within the Gordano Valley include spring issues on valley-side slopes, lake margins and marshes (palustrine tufa) and lake floors (Pedley *et al.* 2003, Viles & Pentecost 2007).

Lime mud (marl) precipitation predominates in association with large bodies of freshwater where it is deposited as sub-horizontal laminites that thin towards the valley axis and downstream of resurgences (Ford & Pedley 1996, Pedley *et al.* 2003). In core TG, TG16 and TG22 may have been deposited in a lacustrine environment. The marl of TG22 in particular forms an extensive feature immediately below peat deposits on Weston Moor, whereas the marl of TG16 is restricted to a more local area (soft light blue clay, Figure 5.5). Similar deposits frequently form in lacustrine or waterlogged valley bottoms (Pedley *et al.* 2003). Marl is associated with large bodies of freshwater, commonly covering much of the lake floor, and may also accumulate locally within the pools, partly from precipitation and partly from material washed in from the surrounding marshy slopes (Ford & Pedley 1996). However, there is no evidence of laminated deposition in either TG16 or TG22 and identification of lacustrine marls is usually carried out by micromorphological fabric

analysis (Freytet & Verrecchia 2002, Preece *et al.* 2007, Candy 2009), not used in this thesis.

Spring issue tufas are extremely local deposits which develop from single or multiple spring resurgences; detrital tufa deposits may be found downstream (Ford & Pedley 1996, Pedley *et al.* 2003). The carbonate concretion in PGA14 which exhibits a concentric, laminar structure focused on the mould of a gastropod shell has similarities to moulds of mollusc shells found in tufa at Marsworth, Buckinghamshire, described by Murton *et al.* (2001), where formation is inferred to have occurred in the low-energy environment of a small limestone spring. Active limestone springs are presently found within the Gordano Valley and tufa deposition could have been from an intermittently flowing calcareous spring located on the Clevedon-Portishead ridge. Alternatively, the concretion may indicate carbonate precipitation associated with a fluctuating, near-surface water table (Preece *et al.* 2007). The tufa clast in PGA3 is probably almost *in situ* as the delicate plant material extending from it would probably have broken off if the clast had experienced significant transport. However, spring issue tufas are never associated with significant bodies of standing water, (Pedley *et al.* 2003) which probably periodically occupied the valley floor.

Palustrine tufas typically occur in lakes with low gradient and low energy margins, in short-lived ponds isolated between siliclastic sediments, in waterlogged valley-bottom situations where line-sourced waters emerge from valley side and bottom aquifers or even in peritidal settings (Alonso-Zarza 2003, Pedley *et al.* 2003). Under these conditions a small fall in water level results in sub-aerial exposure of lacustrine carbonate mud (often with charophytes, molluscs, ostracods, etc.), allowing pedogenic processes to modify the mud (Wright & Platt 1995, Alonso-Zarza 2003). The palustrine environment can include peats, calcareous marsh and ponds, poorly drained slopes and hydromorphic soils (Ford & Pedley 1996, Verrecchia 2007, Viles & Pentecost 2007). The water body is shallow, usually <1 m in depth (Alonso-Zarza 2003, Verrecchia (2007) and small ephemeral pools may persist long enough to allow local accumulations of lime mud and carbonate encrustation of macrophyte and aquatic vegetation (Pentecost 1981, Ford & Pedley 1996). Small phytoherm patches or cushions may develop near pool margins (Ford & Pedley 1996). The tufa clasts in PG6, PGA3 and PGA14, which have the superficial appearance of encrusted bryophyte cushions, may indicate palustrine tufa formation, possibly in a ponded environment where lack of water depth and small flow volume has limited the size of the

cushions (Pedley *et al.* 2003). However, such an interpretation contradicts fluvial sedimentological interpretations, although the tufa clasts could be the result of brecciation of palustrine tufa deposits.

Overall, the presence of groundwater carbonate nodules together with the presence of tufa clasts supports the interpretation that surficial carbonate deposits on gravel clasts represent groundwater carbonates. As palustrine carbonates are sensitive to variations in humidity, carbonate precipitation probably occurred around a shallow water table in a semi-arid or sub-humid climate with marked seasonality, high rates of evaporation and evapotranspiration and intermittent rainfall (Alonso-Zarza 2003). In contrast, absence of carbonate coatings on the gravel clasts of NR5, NR15 and TG14 indicates that either the water table was deeper following deposition of these gravels and/or climate conditions were not conducive to carbonate precipitation.

7.7.4 Geochemical analysis

Geochemical analysis, summarised in Table 7.9, reveals a complex pattern of changes indicating periods of climatic deterioration and amelioration, of organic productivity and landscape stability interspersed with episodes of sparse vegetation cover, increased aridity and landscape instability; for instance the gradual change from a semi-arid climate with sparse vegetation for CGA4 to a wetter climate with increased organic productivity for CGA6 suggests climate amelioration (Walker *et al.* 2003, Walker 2005, Egli *et al.* 2008).

Fluctuating high to very high organic and carbonate content in TG16 to TG22 indicates a period of landscape instability with fluctuating vegetation cover and organic productivity, hydrological carbonate production and carbonate leaching, whereas fluctuating high carbonate and moderate organic content for NR6 to NR9 indicates landscape instability coupled with aridity (Mayle *et al.* 1999, Egli *et al.* 2008).

High carbonate content coincident with high organic content, for example in PG3, indicates landscape stability with organic-rich soil and hydrological carbonate production (Mayle *et al.* 1999, Egli *et al.* 2008), whilst high carbonate content and low organic content, for example in CGA3, indicates carbonate production under semi-arid conditions coupled with loss of organic content through enhanced decomposition or low organic productivity and sparse vegetation (Mayle *et al.* 1999, Walker 2005, Egli *et al.* 2008).

Table 7.9: Summary of post-depositional environments indicated by geochemical analysis

Geochemical evidence	Environment	Units
Fluctuating high to very high carbonate and organic content	Landscape instability, varying vegetation cover and organic productivity, hydrological carbonate production and carbonate leaching	TG16 to TG22
Fluctuating high carbonate and moderate organic content	Landscape instability, some organic productivity, semi-arid conditions	NR6 to NR9
High carbonate content and high organic content	Landscape stability with organic-rich soil and hydrological carbonate production	GV2, PG3, PG5, CM1, CM3, CM4, CM6, CM9, TG4, TG7, TG13, TG15
Increasing organic and carbonate content		NR1 TO NR2, NR13 to NR14, NR18 to NR19
High carbonate content and low organic content	Carbonate production under semi-arid conditions coupled with loss of organic content through enhanced decomposition or low organic productivity and sparse vegetation	GV1, GV3, GV4, GV8, GV9, GV10, PG7, PG8, PGA1, PGA2, PGA3, PGA4, PGA7, PGA9, PGA10, PGA14, CGA1, CGA2, CGA3, CGA4
Moderate carbonate content and low organic content		CGA9, CGA10, CGA12
Low carbonate content and low organic content	Sparse vegetation cover coupled with low organic productivity and strong carbonate leaching due to cool, wet climate conditions	GV5, GV6, CGA13, CGA14, NR11, NR12
High organic and clay content and low carbonate content	Temperate humid climate with vegetation growth	GV7, PGA11, PGA12, PGA13, CGA6, CGA7, CGA8, CGA11, CGB4, CGB5, NR10, NR17, NR20, NR22, NR26, CM5, CM13
Increasing organic and falling carbonate content	Increasing organic productivity and carbonate leaching in a wet, temperate climate	TG1 to TG2, TG5 to TG6, TG10 to TG11
Falling organic and carbonate content	Reduction in vegetation cover and climatic cooling	CGB1 to CGB2, NR15
Decreasing organic content and increasing carbonate content	Reduction in vegetation cover and increased aridity	CGB6, CGB7, CGB13, NR3, NR4, NR5, NR16, NR21, CM10 TO CM11, TG2 to TG3, TG8, TG9, TG12, TG14

Low carbonate content and relatively low organic content, for example in GV5, suggests strong carbonate leaching due to cool, wet climate conditions coupled with low

organic productivity, indicating a cool, wet climate with sparse vegetation cover. (Mayle *et al.* 1999, Walker *et al.* 2003, Walker 2005, Egli *et al.* 2008), whereas relatively high organic and clay content and low carbonate content, as in GV7 for example, indicates a temperate wet climate with vegetation growth (Walker *et al.* 2003, Walker 2005, Egli *et al.* 2008).

TG1 to TG2, TG5 to TG6 and TG10 to TG11 exhibit increasing organic and falling carbonate content indicating increasing organic productivity and carbonate leaching in a wet, temperate climate (Walker *et al.* 2003, Walker 2005, Egli *et al.* 2008), whereas falling organic and carbonate content, for example in CGB1, indicates reduced vegetation cover and climatic cooling (Walker 2005, Egli *et al.* 2008) and decreased organic content coupled with increased carbonate content, for example in CGB6 and TG8, reflects a reduction in vegetation cover and increased aridity (Walker 2005, Egli *et al.* 2008), although in TG8 the high carbonate value may simply reflect the high shell content, masking underlying low carbonate content.

The red to yellowish brown colours of most of the sediments indicates oxygen availability and weathering of sub-aerially exposed surfaces (Ellis & Mellor 1995, Retallack 2001). In contrast, the gley, grey and greyish brown colours of PGA13, PGA15, PGA17, CM4, CM5, CM9 to CM13, TG16 to TG19, TG21 and TG22 indicate waterlogging (Catt 1990), whilst the olive colours of PGA8 and PGA10 indicate periodic waterlogging (Gale & Hoare 1991).

Redness values of ≥ 5.00 for thirty four units indicate possible oxidation of ferrous iron minerals, sub-aerial exposure and pedogenesis (Ellis & Mellor 1995, Retallack 2001), although four units with redness values of ≥ 5.00 (PGA13, PGA15, PGA17 and CM11) are grey coloured. However, for GV1, identified as Triassic mudstone, and GV2, PG7 and PGA14, where lithological analysis has determined a high proportion of brown sandstone clasts, possibly derived from Devonian Old Red Sandstone, the red colour is probably inherited.

Iron staining noted in some units is probably due to ground water fluctuations and the mobilisation and oxidation of iron (Olsen 1998, Ellis & Atherton 2003) or the effects of rhizoturbation resulting in preferential oxidation of sediment (Tucker 2003) and indicates weathering due to the availability of oxygen (Ellis & Mellor 1995, Retallack 2001). For example, iron staining in GV4, PGA14, CGB13, TG8 and TG10 (the latter two units are shown in Figure 6.9) is probably due to ground water fluctuation, whereas that seen in PG3,

PGA11 and CGA11 is probably caused by preferential oxidation associated with rhizoturbation.

Liesegang rings in PGA10 and CGB11 (Figures 6.2 and 6.5) are probably the result of post-depositional variations in the iron oxide and hydroxide content related to progressive weathering, the slow diffusion of pore water through sediment and the precipitation or dissolution of minerals along reaction fronts (Retallack 2001, Tucker 2003). Their deflection around a large carbonate nodule in CGB11 indicates their formation post-dates that of the nodule.

Several units, for example CGA6, CGB7 to CGB11 (Figure 6.5) and NR9 demonstrate black manganese staining of sediment or gravel clasts, manganese cemented pebble concretions and manganese nodules. These indicate shallow phreatic groundwater fluctuations after sediment burial and cycles of manganese mobilisation under reducing and oxidising conditions associated with seasonally wet and dry conditions in a temperate climate regime and sub-aerial exposure (Catt 1990, Olsen 1998, Retallack 2001, Ellis & Atherton 2003, Tucker 2003, Glasser *et al.* 2004).

7.7.5 Pedogenic features

Only twenty one units fail to meet the criterion for organic matter content of 1-4% determined by LOI of silty and sandy material, a reliable indicator of past pedogenic activity (Olsen 1998) or recycling of pedogenic material. However, evidence for soil profile development is rare, being confined to units CGA4 to CGA6, NR13 to NR15 and TG18 to TG22. Some units display superficial characteristics of pedogenesis, but for which supporting evidence is lacking, indicating they are not pedogenetic. For instance, the weak red, yellowish red or reddish brown colours of GV8, CGB1, CGB2, CGB3, CM6, TG1, TG2 and TG3 (redness ratings 10.00 to 3.33) indicate sub-aerial exposure and oxidation of iron minerals under climatic conditions that were possibly as warm as those pertaining today (Catt 1989, Retallack 2001), although iron oxidation may also occur under extremely low temperatures (Francelino *et al.* 2011). GV8 has elevated clay content and a sharp upper boundary which suggests truncation of a soil (Catt 1990); however, organic content is much lower, and carbonate content higher, than for the underlying unit GV7 suggesting local reworking of soil rather than pedogenesis (Catt 1990). Although organic content is elevated in CGB1, CGB2 and CGB3, clay content is low and carbonate content is relatively high,

whilst in TG1, although organic and clay content is elevated, carbonate content is relatively high. In TG2 organic content is elevated but carbonate and clay content is low and in TG3 carbonate content is high, organic content is moderate and clay content is low. Furthermore, redness decreases upwards from CGB1 to CGB3 and TG1 to TG3, indicating these are not pedogenic (Catt 1990).

In CM6, the presence of a void, interpreted as ichnofossil, indicates sub-aerial exposure, whilst drab spots indicate periodic waterlogging. Organic, clay and carbonate content is elevated, suggesting a hydromorphic soil submerged by carbonate-rich groundwater. However, the abrupt start and termination of vertically orientated reed stems suggests high energy transport and reworking of a pre-existing soil, rather than *in situ* pedogenesis.

The very dark greyish brown colour of PGA16 is usually taken to indicate the presence of organic material (Tucker 2003) and the sediment displays a pelletoidal structure consistent with the activity of soil invertebrates under calcareous soil formation (Retallack 2001). However, organic, clay and carbonate content are low, and since it overlies sand with low carbonate content it is more likely to be inwashed material.

However, on the basis of stratigraphical evidence and geochemical analyses, thirty units have been identified as displaying evidence of pedogenesis. These probably formed during periods of reduced or non-deposition during which there was a measure of landscape stability and extensive surface modification of the sediment (Fenwick 1985, Catt 1990, Retallack 2001). The evidence for pedogenesis is outlined below:

CGA2 presents a weak case for pedogenesis; the dark reddish brown colour indicates oxidative conditions, a sub-aerially exposed surface and conditions that were at least as warm as those pertaining today (Catt 1989). There is no evidence for soil profile development, although the sharp planar upper boundary suggests the possibility that upper horizons have been eroded. The elevated levels of carbonate, clay and organic content are weak indications of pedogenesis; the possibility that this is a mature interglacial soil is excluded by the presence of ripples which would have been disrupted by bioturbation.

The light brown colour of CGB4 indicates sub-aerial exposure and oxidation of iron minerals (Retallack 2001). There is manganese mottling, related to incipient soil profiles (Retallack 2001), low carbonate and elevated clay and organic content, indicating weak pedogenesis.

PG3 is calcareous light yellowish brown silt that exhibits a fluvial influence and has relatively high organic and carbonate content consistent with soil formation on the recently exposed surface of a closed basin-type environment (Freytet & Verrecchia 2002, Tucker 2003). Its colour indicates the availability of oxygen and weathering of sub-aerially exposed or emergence surfaces (Ellis & Mellor 1995, Retallack 2001) under a temperate climatic regime. Strong brown mottling, associated with a wood fragment found within the unit, reflects precipitation of iron oxides during fluctuating groundwater conditions. Part of its boundary with PG4 forms a vertical crack which was in-filled during deposition of PG4. The crack is straight sided, so has suffered little subsequent compaction, which rules out formation by syneresis (sediment dewatering) and suggests instead a shrinkage crack (Tucker 2003), indicative of surface exposure and desiccation during a period of non-deposition (Allen 1970). The commonest surfaces for mud cracks are sub-aerially exposed water-saturated sediment surfaces such as the surfaces of dried up pools, lakes and lagoons, abandoned river channels, floodplains and intertidal mud flats (Reineck & Singh 1973). The greenish grey colour of the base of the crack is probably the result of iron reduction through subsequent passage of water through the more permeable sand of PG4.

The yellowish brown to dark yellowish brown colour of CGB12, CM7 and PGA10 to PGA12 indicates sub-aerial exposure and hydration or oxygenation of iron minerals, oxygen availability and weathering of sub-aerially exposed surfaces; iron mottling in CM7 indicates fluctuating groundwater (Ellis & Mellor 1995, Olsen 1998, Retallack 2001, Ellis & Atherton 2003). PGA10 to PGA12 have sharp intervening boundaries, so do not comprise a soil profile. Elevated organic and clay content and low carbonate content for all these units indicate weak pedogenesis, probably on recently exposed surfaces.

PGA13, CM10 and TG6 are greyish brown and grey silts whose colour is usually taken to indicate the presence of organic material (Tucker 2003). In CM10, an ichnofossil and a bioturbation trace indicate sub-aerial exposure (Retallack 2001). All three units have elevated clay content, although only PGA13 and TG6 have elevated organic content and only PGA13 and CM10 demonstrate low carbonate content. Overall, this indicates weak pedogenesis, which for CM10 probably occurred on a recently exposed surface.

The brown colour of CM5 and TG15 indicates sub-aerial exposure and oxidation of iron minerals (Catt 1989, Retallack 2001). In CM5, ichnofossils and a bioturbation trace also indicate sub-aerial exposure (Retallack 2001), organic and clay content is elevated and carbonate content is moderate. Plant stems *in situ* indicate pedogenesis and landscape

stability (Tucker 2003); drab haloes indicate periodic waterlogging and weak pedogenesis in a hydromorphic soil (Retallack 2001). However, although organic and clay content is elevated, carbonate content in TG15 is moderate indicating weak pedogenesis.

PG5 and CM13 are both interpreted as hydromorphic soils. PG5 exhibits relatively high organic and carbonate content and elevated clay content consistent with soil formation on the recently exposed surface of a closed basin-type environment (Freynet & Verrecchia 2002, Tucker 2003), whilst although CM13 also demonstrates elevated organic and clay content, it demonstrates low carbonate content. The greenish grey colour of PG5 suggests it has been subjected to anoxic conditions, whilst the yellow mottling reflects precipitation of iron oxides during fluctuating groundwater conditions under warm temperatures, and its elevated carbonate content indicates submergence by carbonate-rich groundwater. The blue-grey colour of CM13 indicates reducing conditions, again with submergence by groundwater. The presence in CM13 of vertically oriented plant stems suggests *in situ* growth, pedogenesis and landscape stability (Tucker 2003).

According to Retallack (2001) fossil root traces are one of the best criteria for recognising palaeosols in sediments as they provide evidence for better drainage (Retallack 2001). The near-vertical root trace in CGA11 and the fossil root traces in CGB11 are strongly associated with iron mottling due to rhizoturbation resulting in preferential oxidation of sediment around the root traces (Tucker 2003). This indicates conditions of groundwater fluctuation cycles of reducing and oxidising conditions (Olsen 1998, Retallack 2001, Ellis & Atherton 2003). The yellowish brown colour of CGA11 and the brown colour of CGB11 indicate sub-aerial exposure and hydration of iron minerals (Retallack 2001). Elevated clay and organic content and low carbonate content indicate moderate pedogenesis. The sharp upper boundary of CGA11 suggests possible erosion of a horizon. CGB11 contains carbonate nodules, indicating prolonged landscape stability (Marriott & Wright 1993, Tucker 2003).

The reddish brown colour of GV7, PGA5 and NR20, the reddish brown to strong brown colour of CGB10 and strong brown colour of CGB5 indicates sub-aerial exposure and oxidation of iron minerals under climatic conditions that were probably as warm as those pertaining today (Catt 1989, Ellis & Mellor 1995, Retallack 2001), although recent work in the Antarctic by Francelino *et al.* (2011) has shown that iron oxidation may occur even under extremely low temperatures. The sediments display elevated clay and organic content and low carbonate content, suggesting acid soil formation during an interval of

humid, temperate climate and land surface stability (Lowe & Walker 1997, Walker 2005, Egli *et al.* 2008). The clay-enriched silt of GV7 caps a sequence of upward-fining deposits and is consistent with interglacial soil formation on an emerging land surface (Catt 1990, Tucker 2003); its sharp upper boundary suggests erosional truncation of a soil prior to burial (Catt 1990). The presence in NR20 of manganese streaks and iron mottling, the result of fluctuating groundwater conditions, are probably related to incipient soil profiles on recently exposed surfaces (Catt 1990, Retallack 2001, Tucker 2003). In contrast, although CM1 and TG13 also have the reddish brown colour indicative of sub-aerial exposure under warm climatic conditions and organic and clay content is elevated, carbonate content is relatively high, indicating only weak pedogenesis.

The sequences CGA4 to CGA6 and NR13 to NR15 show similarities to soil profiles, with diffuse, gradational boundaries, upward-increasing levels of organic and clay content, a truncated uppermost horizon (Catt 1990, Retallack 2001) and upward-increasing darkness of colour. Alternatively, because manganese nodules and manganese-cemented concretions of pebbles are also found in CGA6, the dark colouration may indicate localised manganese staining related to changes in ground water levels (Catt 1990, Retallack 2001). Similar dark horizons were noted by Gilbertson & Hawkins (1983) in Pleistocene sands at Clevedon Court and Tickenham waterworks, just south of Tickenham ridge, and were considered by those authors to represent incipient soil profiles.

The sharp, irregular upper boundary of CGA6 suggests erosion of upper (organic) horizon; soil is often truncated by erosion prior to burial, and a sharp upper boundary indicates the erosion of one or more soil horizons (Catt 1990). NR13 to NR15 form a sequence of strong brown to dark yellowish brown gravels, whose colour indicates weathering and the hydration or oxygenation of ferrous iron minerals, oxygen availability and weathering of sub-aerially exposed surfaces (Ellis & Mellor 1995, Retallack 2001). Overall, this evidence indicates pedogenesis (Retallack 2001).

The strongest evidence for pedogenesis is found in TG18 to TG22, which form a pedogenic complex of loamy peat (TG18), sandy peat (TG19) and humose (TG20 to TG22) units (definitions follow Catt 1990).

7.8 Geochronology

Two distinct pedogenic episodes are identified from radiocarbon dating. Evidence from NR15 provides a radiocarbon date for the cessation of pedogenesis of 13430 to 13190 Cal BP. This approximates to the timing for the Younger Dryas (Loch Lomond) Stadial and indicates palaeosol formation occurred prior to 13430 Cal BP, during Devensian Lateglacial (Windermere) Interstadial time or earlier.

Evidence from CGA6 provides a radiocarbon date of 22200 to 22000 Cal BP for the cessation of pedogenesis, which approximates to the timing of the maximum extent of the Devensian (MIS 2) BIIS (Bowen *et al.* 2002). This indicates palaeosol formation occurred prior to 22200 Cal BP, possibly during a MIS 3 interstadial or earlier.

A radiocarbon date of 45460 ± 790 BP for mollusc shells in TG8 suggests a mid-Devensian (MIS 3) age. At the time the date was obtained it was assumed that the presence of freshwater molluscs indicated a terrestrial environment, which would be consistent with this date, although this date is close to the limit the technology. However, AAR results from *in situ* mollusc shells from the same unit indicate a late MIS 7 or possibly early MIS 5e age.

The lack of independent geochronological data hampers the determination of an absolute age using amino acid geochronology (Penkman *et al.* 2010) and the paucity of previous data using this methodology is a major constraint on resolution. It is therefore not possible to rule out an early MIS 5e age; a MIS 6 age is also possible, but would be at odds with the faunal and algal evidence. A late MIS 7 age is more likely; the result for alanine (Ala, Figure 6.16) clearly shows the TG8 samples to be MIS 7. Variability of AAR results within the dataset could be because recrystallisation of the aragonite shell potentially plays a significant role in the integrity of the crystal structure as samples get older (Penkman *et al.* 2010). Additionally, the mollusc assemblage indicates fully interglacial conditions, whilst stratigraphically TG8 is overlain by gravel; in areas of tectonic uplift, including the Gordano Valley (Westaway 2010b), increased availability of coarser material is usually associated with cold stages (Lewis *et al.* 2001, Bridgland & Westaway 2008, Vandenberghe 2008).

In order to improve the chronology, OSL dating was used in an attempt to bracket the fossiliferous unit TG8 for which radiocarbon and AAR geochronology of the mollusc shells had been obtained. However, it was difficult to match the stratigraphy of core TG-

OSL to that of core TG in the red light conditions under which core TG-OSL was opened. The OSL dates obtained appear to form a relatively consistent set of results with the exception of sample x3784 which seems younger than the others, although the date is within the quoted error margins of the other samples. The sediment is probably derived from the same source as the underlying sands, and hence the same date; it is possible that the signal from this sediment was not reset, and that the measurement relates to the palaeodose of a previous depositional context (J.-L. Schwenninger, 2011, Pers. comm.). The close dates suggest relatively rapid deposition.

OSL dating usually indicates radiocarbon age underestimation (as reported for example, for Devensian deposits in the Fenland Basin, eastern England, by Briant & Bateman (2009)). In this case, this is probably because radiocarbon dating is at the limit of the technology and is unable to provide an accurate date. However, the OSL dates are not consistent with the AAR geochronology either. Since insufficient bleaching of sediments usually results in OSL age overestimation (Fuchs & Lang 2009, Hülle *et al.* 2009), it is possible that the fossiliferous units represent reworked material incorporated into a Devensian (MIS 5) sequence, as has been inferred for deposits at nearby Shirehampton (Bates & Wenban-Smith 2006) or that this is an instance of OSL dating providing ages that are too young, a phenomenon previously reported by Steffen *et al.* (2009) for samples from southern Peru.

The obvious discrepancy between the radiocarbon date, the OSL dates and the AAR geochronology is puzzling. However, the OSL dates indicate sediment deposition between 107 ka and 48 ka, placing their deposition during a cold climate episode, potentially contradicting the faunal and algal evidence of core TG. Although core TG-OSL did not contain an equivalent of the two fossiliferous units found in core TG, rapid lateral changes in the stratigraphy, also demonstrated for cores PG and PGA (Figures 6.2 and 6.3), less than 1 m apart, mean that it is possible that the OSL dates refer to a later depositional episode than that of the fossiliferous units of core TG and that the OSL and AAR geochronology are probably both correct.

The sedimentary attributes of percussion cores taken from the Gordano Valley have been characterised and their depositional and post-depositional environments interpreted. The sediments reveal polygenetic origins, characteristics inherited from multiple sources and multiple depositional characteristics for the same deposit. In some cases this made it

difficult to assign a primary depositional environment. However, interpretations are still likely to be correct because multiple characteristics often indicate reworking and recycling of pre-existing deposits by multiple transport agencies (Tanner 1991) and identification of these characteristics has improved the sedimentological interpretation.

In the next chapter, depositional and post-depositional environments are integrated to provide the Pleistocene history for each core. Various models for their palaeoenvironmental reconstruction are then discussed and valley-wide Pleistocene palaeoenvironments for the Gordano Valley are reconstructed.